Catena 273 (2026) 110457

Contents lists available at ScienceDirect

Catena

journal homepage: www.elsevier.com/locate/catena

Hydro-thermal controls on soil respiration revealed by continuous measurements at a Mediterranean forest flux site

Lina Fusaro [a,b,*,1], Adriano Conte [c,1], Carlotta Ferrara [d], Tiziano Sorgi [d], Roberto Corsanici [a,e], Silvano Fares [f,b]

[a] Institute of BioEconomy, National Research Council (CNR-IBE), via dei Taurini 19, 00185 Rome, Italy
[b] National Biodiversity Future Center (NBFC), Palermo, Italy
[c] Institute for Sustainable Plant Protection, National Research Council of Italy (CNR-IPSP), Via Madonna del Piano, 10, 50019 Sesto Fiorentino (FI), Italy
[d] Council for Agricultural Research and Economics, Research Centre for Forestry and Wood (CREA-FL), Italy
[e] Department for Innovation in Biological, Agro-food and Forestry Systems (DIBAF), University of Tuscia, Via San Camillo De Lellis snc, 01100 Viterbo, Italy
[f] National Research Council of Italy, Department of Biology, Agriculture and Food Science, Italy

ARTICLE INFO

Keywords:
Soil CO_2 efflux
Hydrological thresholds
Temperature sensitivity
Field capacity
Land–atmosphere carbon exchange
Mediterranean ecosystems

ABSTRACT

Soil respiration (S_R) is a major component of carbon fluxes in forest ecosystems, encompassing contributions from both heterotrophic and autotrophic respiration. In this study, we analysed two years of continuous CO_2 flux measurements obtained using an automated chamber monitoring system to investigate the seasonal drivers of S_R in an evergreen holm oak forest under a typical Mediterranean climate. Soil water content (SWC) thresholds, marking the transition from moisture- to temperature-limited conditions, were determined using a stepwise regression-based approach. The relative importance of each predictor controlling S_R was quantified across the different phases defined by the SWC threshold. Soil moisture exerted a stronger control on S_R than soil temperature. Including a SWC threshold to delineate distinct soil moisture phases improved model performance (R^2 increased from 0.79 to 0.85).

A complementary litter manipulation experiment was conducted to isolate the role of litter surface in modulating soil respiration and to quantify its contribution to soil CO_2 fluxes. Results showed that, under bare-soil condition, the control exerted by soil temperature on S_R below the SWC threshold was further weakened.

To further investigate the threshold effect on the temperature sensitivity of S_R, we calculated Q_{10} values, which confirmed that under the SWC threshold, the response of S_R to temperature is weak. These findings provide important insights for modelling soil respiration in Mediterranean ecosystems exposed to abrupt variations in soil moisture associated with seasonality and climate-change extreme events.

1. Introduction

Carbon fluxes represent a central focus of many research experiments and monitoring activities due to their critical role in climate regulation (Storm et al., 2023). Major international research infrastructures, such as ICOS and LTER incorporate both CO_2 exchange at the ecosystem level and at the soil level in their experimental protocols (Gielen et al., 2017a; Franz et al., 2018). However, measurements of soil CO_2 fluxes are still underrepresented in the main level-1 ecosystem sites. This is a notable oversight since soil respiration (S_R) is a large component of total ecosystem respiration in temperate and boreal forests, depending on season (Brændholt et al., 2018). Accounting for soil CO_2 fluxes is therefore essential for reliable estimates of forest ecosystem responses to climate change and for accurately representing forest–atmosphere interactions in global modelling studies (Phillips et al., 2017).

S_R is a complex biogeochemical process encompassing the combined respiration of autotrophic and heterotrophic components (Bond-Lamberty et al., 2004). The autotrophic component is primarily influenced by gross primary production (GPP), tree physiology, and species composition, including root-associated microbes (Tang et al., 2020). In contrast, the heterotrophic component is driven by the size of the organic matter pool and microbial biomass, including microbial and

* Corresponding author at: Institute of BioEconomy, National Research Council (CNR-IBE), via dei Taurini 19, 00185 Rome, Italy.
E-mail address: lina.fusaro@cnr.it (L. Fusaro).
[1] These authors contributed equally to this work and share first authorship.

https://doi.org/10.1016/j.catena.2026.110457
Received 10 March 2026; Received in revised form 30 May 2026; Accepted 18 July 2026
Available online 28 July 2026

faunal contributions (Hu et al., 2018). This complexity is reflected in the fact that S_R depends on multiple environmental drivers.

Soil temperature (S_T) is widely recognized as a fundamental driver of S_R, influencing the activity of respiratory enzymes in roots and soil microbial biomass, leading to an exponential increase in S_R rates (Johnston and Sibly, 2018). Studies show that S_T enhances S_R across various ecosystems (Yan et al., 2022). However, Tang et al. (2020) reported that global temperature variations explain only up to 25% of respiration, suggesting that S_T may not always be the primary factor controlling S_R. In Mediterranean ecosystems, which frequently experience water scarcity (Lionello et al., 2006; Fusaro et al., 2017), S_R is strongly influenced by water availability, often exhibiting pulse responses to precipitation during prolonged dry periods (Almagro et al., 2009; Matteucci et al., 2015; Conte et al., 2019). These ecosystems show a positive relationship between S_R and S_T during wet periods, which shifts to a negative relationship during dry seasons (Chang et al., 2014). Reductions in precipitation generally suppress S_R, whereas increases have a weaker and irregular positive effect based on precipitation frequency and climate conditions (Du et al., 2023). S_R responds nonlinearly to water availability (Lellei-Kovács et al. 2016, Wang and Feng, 2025), with thresholds and feedback mechanisms that complicate its mechanistic understanding. Soil moisture modulates the temperature sensitivity of S_R, with water-limiting conditions often disrupting expected relationships (Morote et al., 2022). Inferring soil respiration dynamics from spot measurements and extrapolating them through modelling remains methodologically challenging, as S_R responses to temperature and moisture are non-linear and change across moisture regimes (Reichstein et al., 2003; Oyonarte et al., 2012; González-Ubierna et al., 2014). This can lead to an oversimplification of threshold-driven behavior and to uncertainties in attributing underlying mechanisms.

Indeed, case studies within Mediterranean forests have highlighted that soil moisture thresholds significantly modulate the S_R - S_T relationship (Chang et al., 2016; González-Ubierna et al., 2014). These findings underscore the complex interplay between temperature, moisture, and vegetation in regulating S_R and emphasize the need to incorporate soil moisture dynamics and thresholds into models predicting carbon fluxes, particularly in the context of increasing droughts under climate change (Otu-Larbi et al., 2020a, 2020b). Further researches in these ecosystems are crucial for refining our understanding of S_R dynamics and their sensitivity to environmental drivers under changing climatic conditions.

Spatial heterogeneity in roots and litter inputs constrains the generalization of soil respiration fluxes across ecosystems (Kuzyakov and Gavrichkova, 2010). Site-specific studies are therefore essential to detect ecosystem-dependent thresholds and interactions that may be missed by broad-scale analyses (Zhang et al., 2023; Ngaba et al., 2024), while also improving partitioning and upscaling approaches (Subke et al., 2010).

A key parameter for interpreting and modelling S_R is Q_{10}, which describes its temperature sensitivity and varies across ecosystems and seasons (Yan et al., 2019; He et al., 2024). In Mediterranean environments, higher Q_{10} is typically observed during cooler and wetter periods, whereas often decline under summer conditions, when soil moisture becomes a critical seasonal constraint and weakens the temperature–respiration relationship. (Tedeschi et al., 2006; Matteucci et al., 2015; González-Ubierna and Lai, 2019).

Understanding Q_{10} is essential for predicting S_R responses to climate change, as it influences ecosystem carbon fluxes and feedback to atmospheric CO_2 levels. However, significant gaps remain in understanding how Q_{10} is affected by soil moisture, especially in water-limited ecosystems like the Mediterranean. To disentangle S_R drivers and improve our understanding of their components, litter removal experiments provide a valuable approach. The litter layer plays a dual role in S_R dynamics: it serves as a substrate for microbial decomposition, driving heterotrophic respiration, and acts as a physical buffer, modulating soil temperature and moisture conditions (Zhuang et al., 2023).

Litter removal enables partitioning of soil respiration into autotrophic and heterotrophic components (Han et al., 2015). Coupling this experimental approach with modelling improves attribution of seasonal variability and reduces bias in predicting S_R responses to climate change.

In this context, we aim to: (1) identify soil water availability thresholds that regulate S_R dynamics and assess their implications for model performance; (2) quantify how litter removal alters the magnitude and temporal variability of S_R; and (3) investigate the role of soil water content (SWC) in modulating the apparent temperature sensitivity (Q_{10}) of S_R. To address these objectives, we adopted an integrated approach that captures temporal dynamics and threshold-driven responses beyond spot-based measurements, allowing us to quantify the role of key S_R drivers and assess seasonal shifts between autotrophic and heterotrophic contributions.

2. Materials and methods

2.1. Site characteristics

The study site, "Grotta di Piastra" (41°70′ 42″N, 12°35′72″E; hereafter referred to as CPZ), is located in the Presidential Estate of Castelporziano, a protected area of about 6000 ha, near the coast of the Tyrrhenian Sea, ~25 km from Rome, hosting high biodiversity and representing an important peri-urban forest that covers 85% of the entire protected area. In particular, the vegetation at CPZ is representative of a typical old coppice stand dominated by an even-aged evergreen holm oak forest (*Quercus ilex* L.) converted to high forest. The topography is flat, and soil is mainly sandy calcareous phaeozems (Arenic) (93% sand, 4% clay and 3% silt in the first 10 cm) having a mean depth of 0.45 m and low water-holding capacity. The CPZ site is characterized by a meso-Mediterranean climate with a typically hot and dry summer period: on a 15-year basis (from 1996 to 2011), an average of 4 months of drought stress (< 100 mm in the May–August period) was highlighted (Fusaro et al., 2015). The site, equipped with an Eddy Covariance (EC) tower to measure fluxes of CO_2, water vapor fluxes above the forest floor, was included in the Long-Term Ecosystem Research network (LTER – Italy), and in the Fluxnet and ICOS international networks (Fluxnet code IT-Cp2–10.18140/FLX/1,440,233) (Franz et al., 2018; Fares et al., 2025; Gielen et al., 2017a). Following the ICOS protocol (Papale and Nicolini, 2016), the experimental site was divided into five plots arranged around the tower according to the cardinal directions: Plot A (north), Plot D (east), Plot C (south), and Plot B (west). Each plot spans an area of 2000 square meters with a radius of 25 m. In addition to flux measurements, a large set of auxiliary abiotic variables and ecosystem structure are measured under the ICOS protocols (Gielen et al., 2017b). Descriptive statistics of some of these variables are reported in Table 1 to outline the main features of the experimental site. A structural survey was carried out between May and June 2021 on the overall footprint. In each plot five circular litter traps, with a surface area of 0.5 m^2, were randomly placed; the litter traps were emptied monthly and fresh material was taken to the laboratory and dried at 80 °C for leaf biomass determination to have an estimate of the input of organic material to the soil. LAI, m^2/m^2, was assessed utilizing Digital Hemispherical Photography (DHP), which was conducted at nine distinct points within each plot, repeated six times annually. This included two measurement campaigns each in spring and autumn, and one campaign each during summer and winter.

2.2. Experimental design and field measurements

2.2.1. Soil fluxes

S_R was continuously measured using a five-chamber automated system (LI-8250 Multiplexer, LI-COR Biosciences) from May 15, 2022, to

Table 1
Descriptive statistics of forest structural parameters.

	Mean	Max	Min	CV
Forest structure Parameters				
Number of tree (n plot^{-1})	113	168	86	0,416
Basal area (m^2 ha^{-1})	0,081	0,330	0,004	0,100
Diameter at breast height, DBH (cm)	26,87	68,50	8,50	0,66
Tree height (m)	13,83	21,70	7,40	3,49
Leaf Area Idex (m^{2}m^{-2})				
Spring	4,56 ± 0,57	5375	3608	0,126
Summer	3,54 ± 0,28	3889	3100	0,081
Autunm	4,13 ± 0,45	4747	3346	0,111
Winter	3,84 ± 0,39	4360	3232	0,102
Litterfall mass (g m^{-2})				
Spring	46,480	196,44	2,02	0,989
Summer	18,840	118,42	0,98	1186
Autunm	16,180	51,60	0,12	0,65
Winter	14,470	52,60	0,00	0,89

Maximum (Max), minimum (Min), mean (Mean) values, and Coefficient of Variation (CV) are reported for each parameter. Number of trees is expressed per plot; Basal area is expressed per hectare (m^2 ha^{-1}); DBH (cm) indicates diameter at breast height; TH (m) is the trees height in the experimental plot (i.e. tower footprint). LAI indicates leaf area index and is expressed as m^2 leaf area per m^2 ground area; seasonal LAI values are reported as mean ± SD. Litter deposition refers to seasonal dry litter mass per unit ground area (g m^{-2}).

September 2024. The system consisted of five LI-8200-104 Opaque Long-Term Chambers, installed in an area representative of the EC footprint. The chambers were strategically positioned at varying distances from tree trunks (ranging from 1 to 1.5 m) to capture spatial variability in root distribution, following the approach described by Pavelka et al. (2018), thus to remain within a comparable range of potential root influence rather than to explicitly test root-distance effects. The surrounding trees had DBH ranging from 30 to 50 cm, ensuring a relatively uniform contribution of autotrophic respiration related to roots to the total S_R across chambers. The automatic soil respiration chambers were installed within the ICOS Continuous Plots located around the eddy-covariance tower (CP_A, CP_B, CP_C, and CP_D). These plots were not considered as experimental treatments, but as monitoring plots representative of spatial variability within the tower footprint. To assess the effect of the surface litter layer, a local paired comparison was established within CP_B. One chamber was maintained under natural litter-covered conditions (S_{Rref}), whereas surface litter was carefully removed from the paired chamber to obtain bare-soil respiration (S_{Rb}). The paired chambers were positioned close to each other, at comparable distance from nearby tree trunks and under similar microsite conditions, to minimize differences in root influence. This comparison was intended to assess the local effect of litter presence/removal, not to provide a fully replicated experiment across all plots. This setup allowed a paired comparison of soil CO_2 efflux with and without surface litter, providing an estimate of the surface-litter-related contribution to soil respiration. Because S_{Rb} still includes heterotrophic CO_2 production from soil organic matter decomposition, and both S_{Rref} and S_{Rb} include root respiration, this comparison should not be interpreted as a complete partitioning between autotrophic and heterotrophic respiration (Aranda-Barranco et al., 2025).

Hereafter, S_R refers to the average soil respiration measured across the four chambers where the litter layer was left intact. One month prior to the start of measurements (April 2022), five polyvinyl chloride (PVC) rings (20.3 cm in diameter, 11 cm in height) were installed at least 3 cm into the soil. This installation optimized the interface with the litter layer while minimizing root disturbance and cutting. The depth of each collar from the soil surface to its top edge was recorded to precisely calculate the total chamber volume for flux computations. S_R was continuously measured using the automated chamber system: each measurement cycle lasted 180 s, including a 30-s pre-purge and a 30-s post-purge to eliminate residual gases inside the chamber and the system. Two records for each hour were recorded. Flux data were processed with SoilFluxPro® (version 4.0.1, LI-COR Biosciences, Lincoln, NE, USA) using a linear fitting for flux calculations.

2.2.2. Environmental variable measurements

Soil temperature (S_T, °C; Barnant Co., Barrington, IL, USA) and soil water content (SWC, %; Theta Probe ML2x, Delta-T Devices, Cambridge, UK) were monitored at 10 cm depth below the soil surface using the environmental sensor network established within the ICOS Continuous Plots. The automatic soil respiration chambers were co-located as closely as possible with the corresponding S_T and SWC sensor profiles, so that these measurements represented the local hydro-thermal conditions associated with the measured soil CO_2 efflux. Sensors were not installed inside the chamber collars to avoid disturbing the soil volume used for CO_2 flux measurements. This configuration ensured consistency with the standardized ICOS monitoring framework and allows future integration of chamber-based fluxes with the long-term environmental dataset available at the site. The acquisition protocol included four measurements per hour for each chamber, ensuring high temporal resolution of the collected data. In addition to S_T and SWC, all the environmental variables were acquired from ICOS data portal; in particular, air temperature (T_a, °C), relative humidity (RH, %), Shortwave incoming radiation (SW, W m^{-2}), wind speed (WS, m s^{-1}), wind direction (WD, °), vapor pressure deficit (VPD, mbar), air pressure (PA, kPa), Rainfall (P, mm), Soil heat flux (G, W m^{-2}) were used (Fares et al., 2025).

2.3. Data analysis

To ensure dataset reliability and minimize the influence of measurement artefacts, an Interquartile Range (IQR)-based outlier-screening procedure was applied to the half-hourly soil CO_2 flux records as a quality-control step prior to aggregation to daily means. The filtering was implemented separately for each season (winter, spring, summer, and autumn), thereby accounting for seasonal differences in soil respiration magnitude and variability.

To identify extreme half-hourly flux values potentially associated with measurement artefacts, unstable chamber readings, or transient disturbances, the first and third quartiles (Q1 and Q3) were computed, and values lying below Q1–3 × IQR or above Q3 + 3 × IQR, where IQR = Q3 - Q1, were identified as extreme outliers and excluded from the subsequent analysis. Although very short-lived and isolated post-rainfall peaks may occasionally have been flagged as outliers, the season-specific IQR filtering reduced the risk of systematically removing recurrent post-rainfall increases in soil CO_2 efflux. In total, 324, 95, and 44 half-hourly records were removed in 2022, 2023, and 2024, respectively. After quality control, daily mean soil respiration (S_R) values were calculated for each chamber and used as the temporal reference for all subsequent modelling analyses, including the estimation of apparent temperature sensitivity (Q_{10}).

The sensitivity of S_R to S_T was computed through regression analysis fitting data with an exponential equation proposed by Vant'Hoff:

$$SR = ae^{bT}$$

Where T is soil temperature (°C), a and b are fitted parameters. The apparent Q_{10} was then calculated from the coefficient b of regression Eq. (1), as follows

$$Q_{10} = e^{10b}$$

Q_{10} was calculated using a 60-day moving window shifted at 7-day intervals, following Matteucci et al., 2015, to descriptively visualize its relationship with SWC. The differences between S_{Rref} and S_{Rb} across seasons were analysed by applying the Shapiro-Wilk normality test (Shapiro and Wilk, 1965) to check the normality of the data distribution, followed by a non-parametric statistical Wilcoxon test. Statistical analyses were performed using R software (version 4.4.2).

2.3.1. Soil respiration modelling

The modelling framework was applied at two complementary levels. A first model, representative of the entire forest stand, was developed by averaging S_R values from the four chambers in which no manipulative experiment was conducted (i.e. with the litter layer left intact), thereby providing a site-representative model parametrization that captures the spatial variability sampled across the ICOS Continuous Plots around the eddy-covariance tower. The same procedure was applied to the paired chambers in CP_B to assess whether litter presence or removal locally modified soil respiration responses to environmental drivers. This parameterization, unlike the stand-level model, is not representative of the entire forest but is specific to the individual CP_B and is aimed at isolating the effect of litter on the observed fluxes. For both modelling levels, thresholds and associated regression models were optimized iteratively. To account for changes in environmental conditions that may limit or stimulate S_R, the model was structured around distinct response domains taking into account (i) the mean daily volumetric soil water content at 10 cm depth (THR_{SWC}), (ii) the minimum daily cumulative precipitation capable of inducing a CO_2 pulse upon soil rewetting and the duration (in days) of the rewetting effect on S_R (THR_P). Thresholds controlling soil respiration (S_R) responses to SWC and P were optimized through an iterative, data-driven procedure. Thresholds parameter optimization was performed via an exhaustive grid search over predefined ranges. Specifically, precipitation thresholds were tested between the maximum and the minimum observed value (step = 0.1 mm), SWC thresholds between the SWCmin and SWCmax (step = 0.1%), and pulse durations of 0 or 1 day. For each parameter combination, precipitation events exceeding THR_P were identified, and all days included within the corresponding time window were classified as "rain pulse conditions". Remaining observations were further partitioned into high- and low-SWC subsets based on THR_{SWC}. Because each threshold combination altered both the size and composition of these subsets, regression models were fully re-estimated at every iteration. Separate multiple linear regression models were fitted for rain pulse, high-SWC, and low-SWC conditions. For each subset, model selection was performed using a bi-directional stepwise procedure based on Akaike's Information Criterion (AIC, k = 2) implemented in the *step* function (Hastie and Pregibon, 1992; Venables and Ripley, 2002) of the *stats* R package (R Core Team, 2025) . Starting from the full model, including the whole initial pool of ten candidate predictors (i.e. SW, PA, P, WS, WD, RH, VPD, S_T, SWC and G) variables were iteratively added or removed until no further reduction in AIC was achieved. At each iteration, the Variance Inflation Factor (VIF) was computed to diagnose multicollinearity (Miles, 2014), and predictors with VIF > 2.5 were sequentially removed until all retained predictors met the criterion (Zuur et al., 2010).

Model performance was evaluated using the residual standard error (RSE). For each threshold combination, the mean RSE of the max and min SWC submodel was computed and stored; the optimal parametrization was identified as the one minimizing the RSE. Model development and threshold optimization were conducted on 80% of the dataset, while the final model was validated on the remaining 20%.

The relative weights analysis (RWA) of significant environmental variables from each model was quantified by partitioning R^2, averaged over predictor orderings, following Lindemann et al. (1990), using the *relaimpo* R package (Groemping, 2006). Coefficients of the final stepwise regression models for each water-availability condition are reported in Supplementary Material (Table SM1).

3. Results

3.1. The temporal evolution of the main environmental variables and soil respiration

Air temperature (T_a) and soil temperature (S_T) show a strong annual cycle, with minima in winter (≈ 0–5 °C) and peaks above 25 °C in summer (Fig. 1). T_a peaks differently based on the years: in June, July and August in 2022, 2023 and 2024 respectively; 2024 stands out for the maximum temperature reached in summer (27.2 ± 3.6). S_T follows the same ordering with higher values in August 2024 (25.8 ± 1.2). Rainfall events are concentrated mainly in fall and, to a lesser extent, spring, with markedly dry summer periods, especially in 2023, the driest year with total summer precipitation of 75.4 mm, compared to 143.45 mm in 2022 and 287 mm in 2024. During summer, SWC showed a similar seasonal pattern among years, with prevailing daily mean values around or below 6%, indicating persistently dry soil conditions. Short-term increases occurred after rainfall events, in some cases approaching values around 10%. In autumn, SWC progressively increased with the return of seasonal precipitation, showing a more sustained recovery compared with the short-lived summer responses.

3.2. General modelling soil respiration

The optimization procedure was run for S_R (mean values for chambers with litter). As for S_R, the model yielded threshold values of 9.6% for SWC (THR_{SWC}), 1.3 mm for minimum cumulative precipitation and 1 day for the rewetting period (THR_P). Based on these thresholds, the model achieved R^2 values of 0.786, 0.847 and 0.232 for simulating respiration under SWC < THR_{SWC} or SWC ≥ THR_{SWC}, and during soil rewetting (Precipitation> THR_P), respectively (Table S1).

The relative importance of predictors (RWA) for each model is reported in Fig. 2. Under SWC < THR_{SWC}, SWC and soil temperature were the most important predictors, accounting for 59.46% and 23.57% of model variability, respectively. Under SWC ≥ THR_{SWC}, S_T and shortwave radiation were the most important predictors, accounting for 68.54% and 24.94% of the variability in S_R, respectively. Although statistically significant ($p < 0.05$), the other predictors contributed less than 10% to explaining the variability in both models (Table S1). Under rain pulses conditions (THR_P), the predictors identified by the stepwise procedure were S_T and wind speed accounting for 53.1% and 46.9% of R^2.

Across all chambers with litter, the relationship between observed and simulated soil respiration (S_R) indicates a good agreement (Fig. 3, upper panel). The linear regression shows a slope of 1.02 and an intercept close to zero (0.03), with a coefficient of determination of R^2 = 0.72, demonstrating that the model captures a substantial fraction of the observed variability. Over the period from May 2022 to September 2024, simulated values are displayed according to the model domain from which they were derived (Fig. 3, lower panel). Overall, discrepancies between observed and simulated S_R apperaed associated with specific thermo-hydrological combinations rather than being uniformly distributed across the time series. Model overestimation occurred mainly under two contrasting conditions: at low S_T classes, approximately 6–10 °C, when SWC was relatively high, up to about 14% (≥ THR_{SWC}) with estimates exceeding observations up to +2.52 μmol CO_2 m^{-2} s^{-1}, and at high S_T classes, approximately 26–28 °C, when SWC was low, around 6–8% (< THR_{SWC}) with overestimation up to +3.53 μmol CO_2 m^{-2} s^{-1}. Conversely, model underestimation was more evident under warm conditions combined with low-to-moderate SWC, particularly at S_T classes around 18–26 °C and SWC above the threshold (between 10 and 14%). The strongest negative deviations occurred within this range; for example at S_T = 20 °C or 24 °C and SWC = 12% underestimation reached −6.00 μmol CO_2 m^{-2} s^{-1} and − 7.14 μmol CO_2 m^{-2} s^{-1} respectively. Rainfall-pulse conditions showed more variable errors, consistent with the lower performance of the pulse model that underestimate S_R.

3.3. Assessment of litter contribution to S_R

The same modelling scheme was applied to S_{Rref} and S_{Rb} (coupled chambers in CP_B to distinguish litter-covered from bare soil), allowing a direct comparison of fluxes and isolating the component related to litter

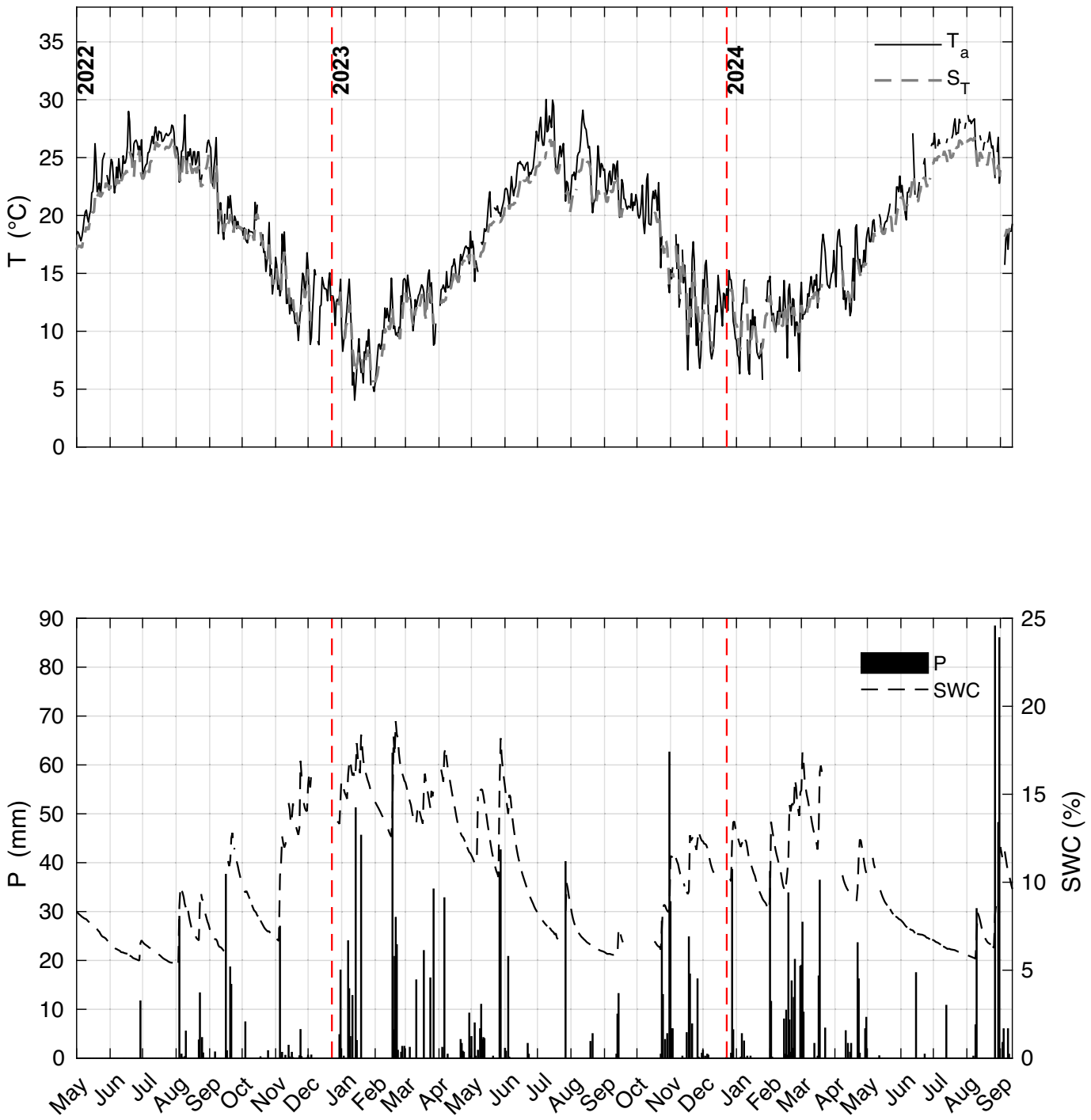

Fig. 1. Time series of environmental parameters referred to the experimental period: 2022–2024: (a) Mean daily air temperature at 21 m height (T_a, °C), mean soil temperature measured at 10 cm depth (S_T, °C); (b) Total daily precipitation (P) and mean daily soil water content measured at 10 cm depth (SWC, %).

presence. Model results are shown in Figs. 4–6 and in supplementary Materials for both chambers (Table S2). In this case, the optimization procedure yielded different thresholds: for S_{Rref}, 10.6% for THR_{SWC}, 2.4 mm for minimum cumulative precipitation and 1 day for THR_P; for S_{Rb}, 7.5% THR_{SWC}, 2.7 mm, and 1 day for THR_P. When SWC fell below THR_{SWC}, for both S_{Rref} and S_{Rb}, SWC and S_T accounted for the largest contributions to R^2 with different weights: 42.52% and 38.03%, respectively, in S_{Rref}, leading to a good accuracy of the model (R^2 = 0.718); 53.35% and 19.17%, respectively in S_{Rb}, with model accuracy of 0.719 (Fig. 4a, d).

Under SWC ≥ THR_{SWC}, the predictors of S_{Rref} identified by the stepwise procedure were S_T, PA, SW and G, with a relative contribution to R^2 of 51.8, 18.7, 16.7, and 10.1%, respectively, leading to a model accuracy of 0.827. In S_{Rb}, RWA revealed an even stronger role of S_T, and SW, with relative contributions to R^2 of 66.54%, and 16.73%, respectively leading to R^2 = 0.72 (Fig. 4 b,e).

Under rain pulses, the most important variables are WS, RH and G with relative contributions to R^2 of 39.4, 34.9 and, 18.2%, respectively; the model showed low accuracy especially in S_{Rref} (R^2 = 0.33). S_{Rb} showed higher accuracy (R^2 = 0.63), with S_T, VPD, WS, G and RH identified as important predictors, with relative contributions to R^2 of 55.9, 18.31, 11.31 and 10.1% respectively (Fig. 4 c, f).

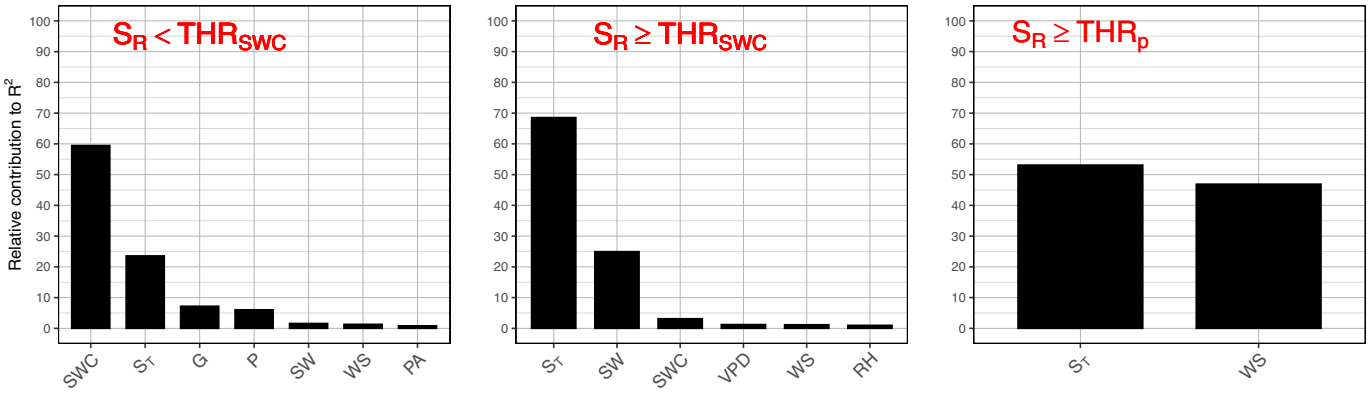

Fig. 2. Relative importance of predictors for S_R under a) SWC < THR_{SWC} b) SWC ≥ THR_{SWC}, and c) rain pulse (THR_P). The variance explained by each predictor is expressed as a percentage of the model's R^2. The predictors included in the analysis are arranged in decreasing order of their contribution: soil water content (SWC, %); S_T, Soil Temperature (°C); G, soil heat flux (W m^{-2}); P, precipitation (mm); SW, short wave (W m^{-2}), WS, wind speed (m s^{-1}), and PA, atmospheric pressure (kPa).

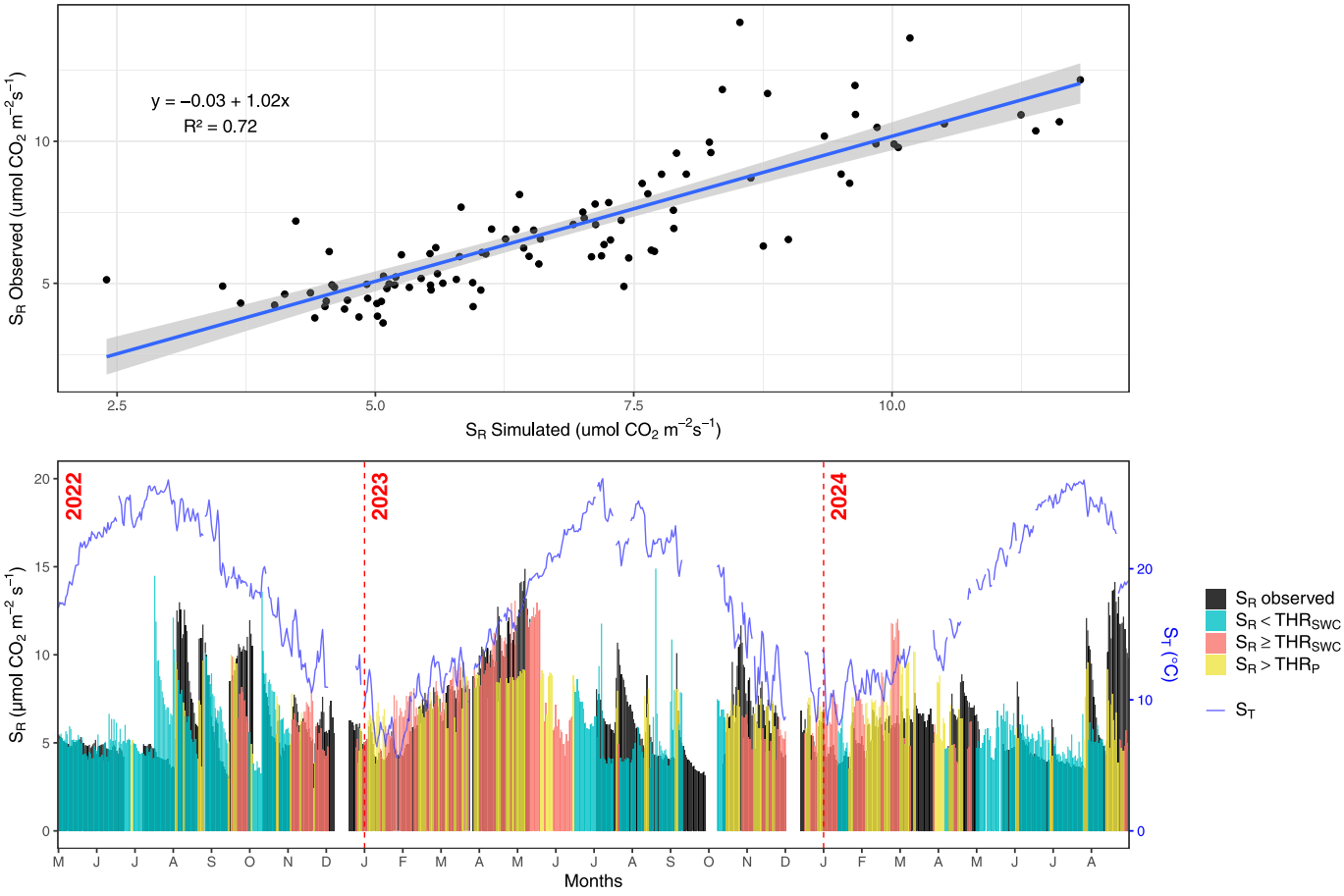

Fig. 3. Upper panel: relationship between observed and simulated daily mean S_R, with linear regression fit shown as a blue line, 95% confidence interval as a shaded area, and corresponding regression equation and R^2. Lower panel: time series of observed and simulated daily mean S_R from May 2022 to September 2024. Observed S_R is shown in black, while simulated S_R values are colour-coded according to the model domain from which they were derived: cyan indicates S_R estimates for SWC < THR_{SWC}; red indicates S_R estimates for SWC ≥ THR_{SWC}; and yellow indicates S_R esteemed under rainfall-pulse conditions. Soil temperature (S_T) is shown on the secondary y-axis as a blue line. Vertical dashed red lines indicate the transition between years. (For interpretation of the references to colour in this figure legend, the reader is referred to the web version of this article.)

Although statistically significant ($p < 0.05$), the remaining predictors contributed <10% to explaining the variability in both models (Table S1).

In all years, both S_{Rref} and S_{Rb} increased during spring, peaked in summer, and declined toward fall and winter in both observed and simulated time series. Linear regression for S_{Rref} yielded a slope of 0.94 and an intercept of 0.61, with a good coefficient of determination (R^2 = 0.62) (Fig. 5, upper panel), indicating that the model reproduced a substantial fraction of the observed variability but with greater dispersion at higher flux values. Over the study period, simulated S_{Rref}

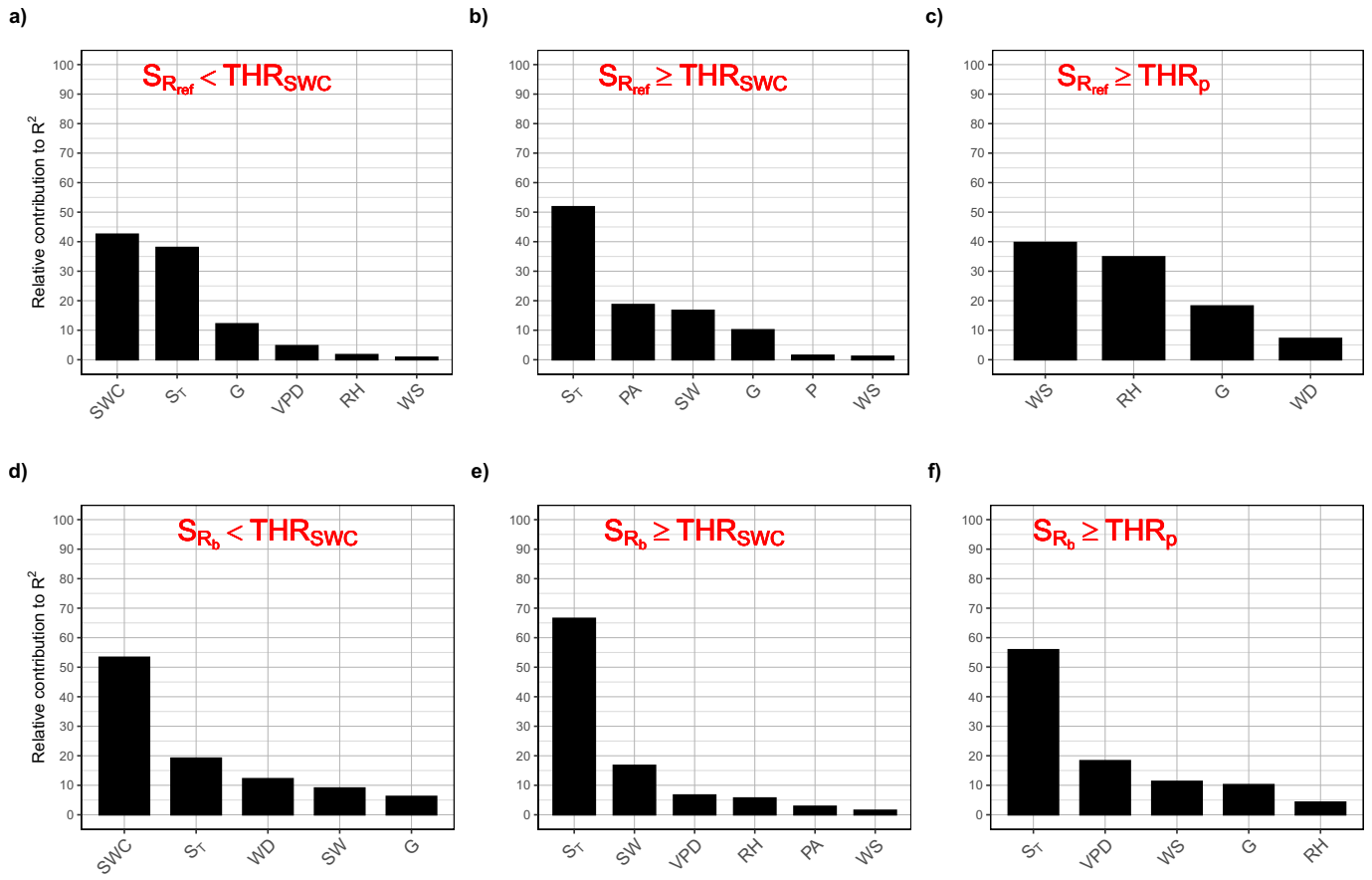

Fig. 4. Relative importance of predictors for CO_2 release measured by a single chamber in plot B, in the case of litter presence (S_{Rref}) or in the case of litter absence (S_{Rb}) under SWC a) lower (a, d), higher (b, e) than threshold, and rain pulses (c, f). The variance explained by each predictor is expressed as a percentage of the model's R^2. The predictors included in the analysis are arranged in decreasing order of their contribution: soil water content (SWC, %); S_T, Soil Temperature (°C); G, soil heat flux (W m^{-2}); P, precipitation (mm); SW, short wave (W m^{-2}), WS, wind speed (m s^{-1}), and PA, atmospheric pressure (kPa).

generally reproduced the main seasonal dynamics, with increasing fluxes during spring and summer and lower values during winter and late dry-season periods (Fig. 5, lower panel). Model overestimation occurred mainly under relatively low-to-intermediate S_T classes, approximately 8–14 °C, when SWC was above the S_{Rref} threshold, with overestimations up to +9.68 μmol CO_2 m^{-2} s^{-1} at S_T = 10 °C and SWC = 12%, and + 7.91 μmol CO_2 m^{-2} s^{-1} at S_T = 8 °C and SWC = 18%. Conversely, model underestimation was more evident under warm conditions, particularly when S_T exceeded approximately 22 °C and SWC was below or close to the S_{Rref} threshold. The strongest negative deviations occurred at S_T = 24 °C and SWC = 10%, with underestimation reaching −9.49 μmol CO_2 m^{-2} s^{-1}, and at S_T = 26 °C and SWC = 10%, with underestimation reaching −8.04 μmol CO_2 m^{-2} s^{-1}.

In rainfall-pulse conditions, model deviations varied in both direction and magnitude according to the seasonal hydro-thermal context. Overestimation was more evident during cooler winter or early spring pulses, whereas underestimation occurred mainly during warmer rewetting phases following summer drought. This pattern is consistent with the lower performance of the rainfall-pulse model. S_{Rb} showed a slope of 0.95, intercept of 0.59 and R^2 = 0.66. For most S_T–SWC combinations, a relatively good model performance across a broad range of hydro-thermal conditions was observed. Model overestimation occurred mainly when SWC exceeded the threshold. The largest positive deviations were observed at S_T = 22 °C and SWC = 18%, with overestimation up to +7.41 μmol CO_2 m^{-2} s^{-1}. Conversely, model underestimation was less frequent but became evident during warm periods, especially when high S_T coincided with low-to-moderate SWC. The strongest negative deviations occurred at S_T = 24 °C and SWC = 10%, reaching −7.45 μmol CO_2 m^{-2} s^{-1}. These underestimations were particularly visible during the 2024 growing season, when observed S_{Rb} peaks were not fully reproduced by the model. Overall, S_{Rb} showed fewer large deviations and a stronger agreement under intermediate hydro-thermal conditions than S_{Rref}. This more stable behavior was also reflected in the rainfall-pulse domain in which S_{Rb} deviations were generally smaller than those observed for $S_{Rref,}$. This indicates that rainfall-pulse responses remained difficult to reproduce, but were less variable under bare-soil conditions than under litter-covered conditions.

3.4. Soil fluxes differentiation: Litter exclusion effect

The seasonal dynamics of soil respiration measured in CP_B, showed a consistent pattern between the two treatments, with both S_{Rref} and S_{Rb} peaking in spring and summer and reaching their minimum in winter (Fig. 7). Respiration under litter was generally higher across all seasons.

Mean S_{Rref} values ranged from a minimum of 5.43 ± 1.29 μmol m^{-2} s^{-1} in winter to a higher mean value of 7.79 ± 2.68 μmol m^{-2} s^{-1} in fall. Data were more tightly clustered around the mean in winter and more dispersed in summer. S_{Rb} ranged from a minimum of 1.84 ± 0.72 μmol m^{-2} s^{-1} in winter to a higher mean value of 4.89 ± 2.02 μmol m^{-2} s^{-1} in summer; variability was lower in spring and more pronounced in summer and fall.

Throughout the measurement period, S_{Rref} was consistently and significantly higher than S_{Rb}, highlighting the additional contribution associated with surface litter presence and litter decomposition to total soil CO_2 efflux. The difference between S_{Rref} and S_{Rb} was most pronounced in spring and fall, while the offset was less evident in summer, possibly due to reduced moisture availability limiting microbial activity. In winter, both S_{Rref} and S_{Rb} decreased sharply, reflecting the combined

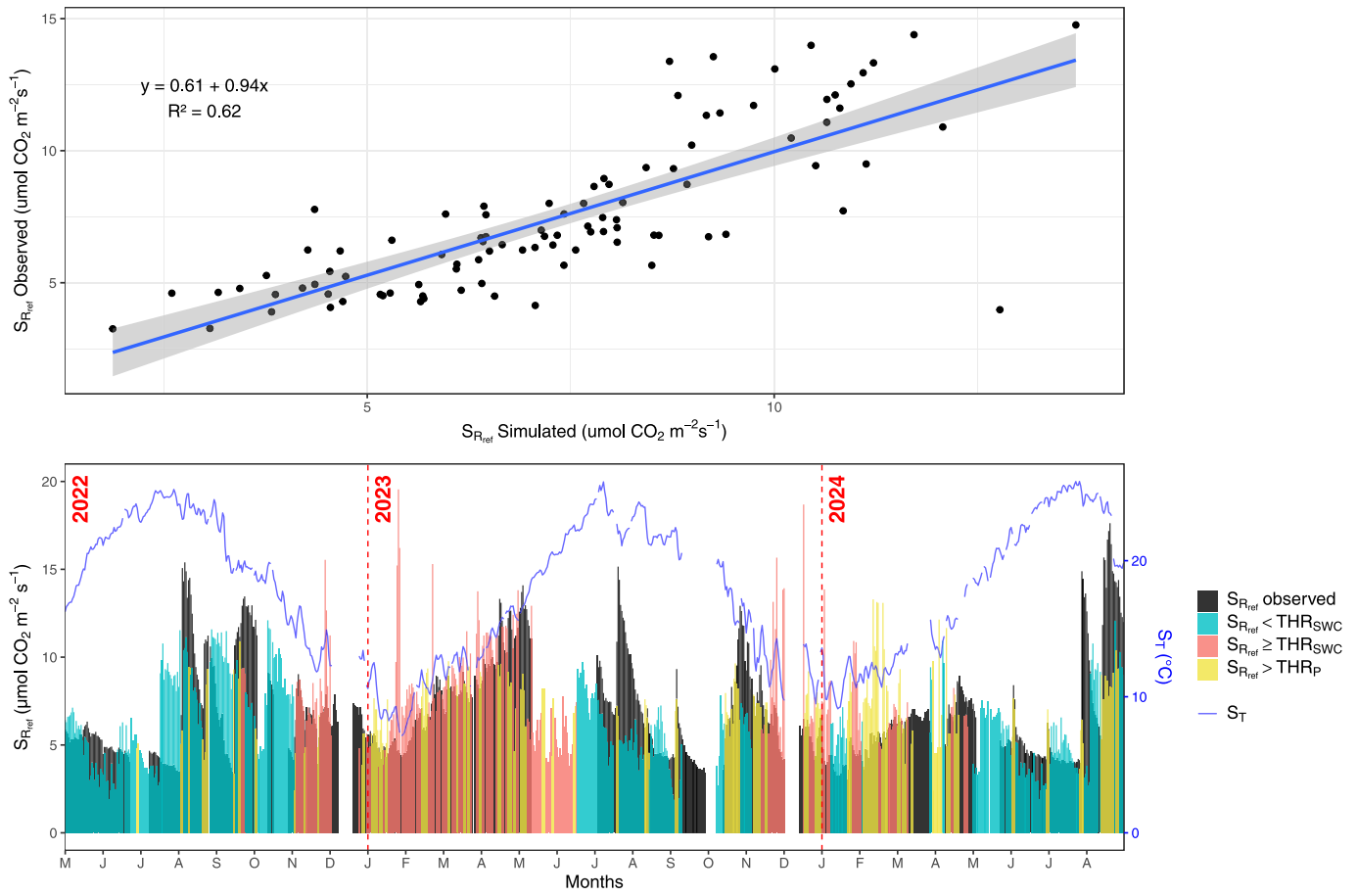

Fig. 5. Upper panel: relationship between observed and simulated daily mean S_{Rref}, with linear regression fit shown as a blue line, 95% confidence interval as a shaded area, and corresponding regression equation and R^2. Lower panel: time series of observed and simulated daily mean S_{Rref} from May 2022 to September 2024. Observed S_{Rref} is shown in black, while simulated S_{Rref} values are colour-coded according to the model domain from which they were derived: cyan indicates S_{Rref} estimates for SWC < THR_{SWC}; red indicates S_{Rref} estimates for SWC ≥ THR_{SWC}; and yellow indicates S_{Rref} estimeed under rainfall-pulse conditions. Daily mean Soil temperature (S_T) is shown on the secondary y-axis as a blue line. Vertical dashed red lines indicate the transition between years. (For interpretation of the references to colour in this figure legend, the reader is referred to the web version of this article.)

effects of low temperatures and reduced biological activity.

The exponential relationship observed between soil respiration and soil temperature was analysed (Fig. 8). For S_{Rref}, including all data together, the temperature sensitivity (Q_{10}) was 1.1 and the exponential relationship explained only a limited fraction of the variance (R^2 = 0.02); such values are common in field respiration datasets where multiple environmental drivers operate. When the dataset was filtered using the iteratively determined threshold (SWC = 10.6%), the relationship between S_{Rref} and S_T diverged. At SWC > 10.6%, the exponential relationship strengthened substantially, and the estimated Q_{10} increased to 2.66, reflecting a higher temperature sensitivity under moist conditions (Fig. 8, left panel). For SWC < 10.6%, the exponential fit was weak and not significant (p = 0.141) (Table 2). In contrast, for S_{Rb}, the dependence on temperature was consistently stronger. When all data were included, the model yielded Q_{10} = 1.71 (p = 0.001), indicating a clear exponential increase of respiration with temperature. Restricting the S_{Rb} dataset to SWC > 7.5% further enhanced both the goodness of fit (R^2 = 0.66) and the temperature sensitivity (Q_{10} = 2.51), suggesting that water availability amplifies the thermal response of S_{Rb}. Conversely, at SWC < 7.5%, the relationship between S_{Rb}, and S_T weakened considerably (R^2 = 0.04), and the derived Q_{10} decreased (1.43). A concise comparison of the main SWC and precipitation thresholds, model R^2 values, and apparent Q_{10} estimates across the general S_R, S_{Rref} and S_{Rb} dataset, is provided in Table S3. Building on these threshold-specific results, Fig. 9 shows the relationship between moving-window apparent Q_{10} estimates, calculated following Matteucci et al. (2015), and SWC. The pattern suggests a moisture-dependent response tending toward saturation, with the model-derived SWC threshold separating two distinct response regimes.

4. Discussion

4.1. Modelling approach

The large spatial variability of S_R reported for temperate forests, within which Mediterranean ecosystems are included, highlights the intrinsic heterogeneity of these systems. With coefficients of variation averaging around 30% in warm temperate regions, spatial differences in S_R can substantially influence site-level carbon estimates (Cai et al., 2023). This highlights the value of well-characterized case studies, which can help disentangle the most relevant drivers and provide the mechanistic understanding needed to upscale S_R estimates more reliably across heterogeneous forest landscapes. Building on this rationale, our analysis did not simply reiterate the well-established role of temperature as a primary driver of soil respiration but explicitly tested whether distinct soil water content thresholds can be identified at our site. Using a data-driven model selection approach, we found that soil respiration responds to temperature only within specific moisture ranges, whereas outside these ranges soil water availability becomes the dominant limiting factor.

These findings are consistent with previous studies reporting threshold-driven shifts in the relative importance of temperature and

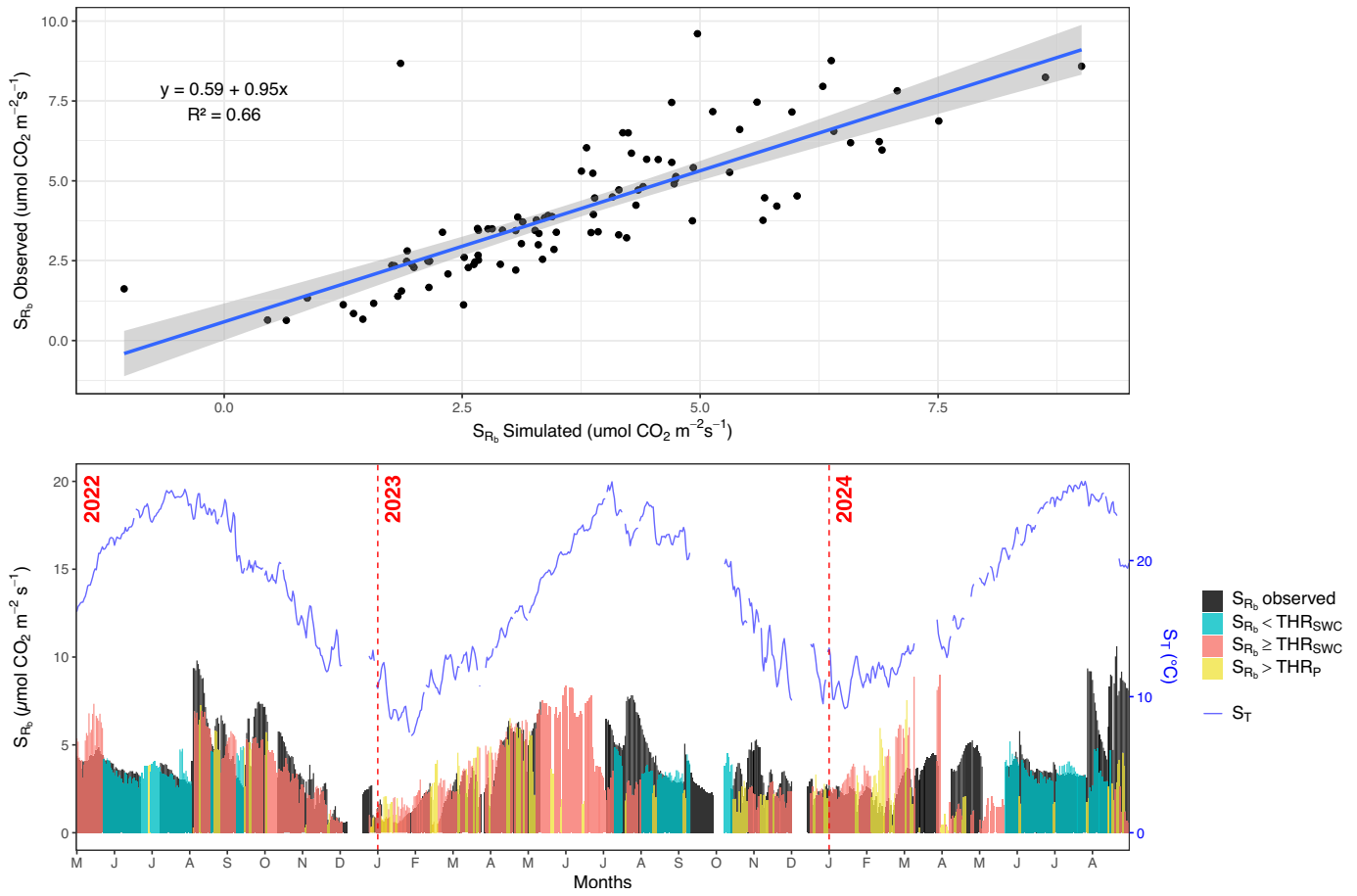

Fig. 6. Upper panel: relationship between observed and simulated daily mean S_{Rb}, with linear regression fit shown as a blue line, 95% confidence interval as a shaded area, and corresponding regression equation and R^2. Lower panel: time series of observed and simulated daily mean S_{Rb} from May 2022 to September 2024. Observed S_{Rb} is shown in black, while simulated S_{Rb} values are colour-coded according to the model domain from which they were derived: cyan indicates S_{Rb} estimates for SWC $<$ THR_{SWC}; red indicates S_{Rb} estimates for SWC $\geq$ THR_{SWC}; yellow indicates S_{Rb} estimeed under rainfall-pulse conditions. Daily mean Soil temperature (S_T) is shown on the secondary y-axis as a blue line. Vertical dashed red lines indicate the transition between years. (For interpretation of the references to colour in this figure legend, the reader is referred to the web version of this article.)

moisture in regulating soil respiration (Lellei-Kovács et al., 2011; Wang and Feng, 2025), but extend this framework by demonstrating that soil moisture thresholds themselves are not fixed and can vary with surface organic conditions. In particular, the higher threshold observed under litter-covered conditions compared to bare soil suggests that litter presence modifies the hydrological and biophysical context under which soil respiration transitions between moisture and temperature-limited regimes. Soil physical conditions regulate water retention and pore connectivity, influencing microbial access to moisture and oxygen, while organic inputs such as litter modify near-surface microclimates that in turn modulate the moisture sensitivity of respiration (Hao et al., 2025). The occurrence of such variable thresholds supports the view that soil respiration responses reflect integrated responses of biotic and abiotic factors, emerging from site-specific interactions among soil physical properties, substrate availability, and microclimatic conditions, rather than reflecting a single, universal moisture constraint (Dacal et al., 2022; Bond-Lamberty et al., 2024). These findings highlight the ability of the threshold approach to identify locally meaningful hydrological boundaries that regulate the transition between moisture-limited and temperature-responsive respiration. Although the resulting thresholds are inherently site-specific, reflecting local soil and environmental constraints, the approach itself is transferable and can be applied across seasonally water-limited ecosystems where soil hydraulic properties strongly constrain soil CO_2 efflux. This interaction is especially relevant in Mediterranean ecosystems, where strong seasonal drought frequently imposes moisture limitation: below threshold soil water content, microbial activity is primarily constrained by water availability, whereas above the threshold, temperature becomes the dominant driver of respiration, consistent with previous observations (Lellei-Kovács et al., 2011).

From a modelling perspective, these results highlight the limitations of assuming a single soil moisture threshold or a constant temperature sensitivity across contrasting surface conditions. Our findings indicate that litter presence alters not only the magnitude of soil respiration but also the functional relationship between respiration, soil moisture, and temperature, implying that models neglecting such context dependency may lead to biased parameterization. Although incorporating moisture thresholds or phase-specific representations of soil respiration increases model complexity, such approaches appear necessary to realistically capture soil carbon dynamics under projected warming and increasing water scarcity, particularly in Mediterranean forest ecosystems (Almagro et al., 2025).

In this study we empirically identified a SWC threshold of ~10% below which soil moisture plays a dominant role, compared to other environmental covariates at our study site (SM1, Fig. 2). By splitting the dataset according to this threshold, we were able to examine each subset separately and better identify the drivers that regulate S_R rates. Support for a threshold-based hydro-thermal regulation of soil respiration has also been provided by Rodríguez et al. (2023) showed a similar threshold-based behavior when modelling S_R as a function of S_T and SWC in a holm oak forest characterized by a continental Mediterranean climate: they identified a S_T threshold around 17–18 °C, associated with

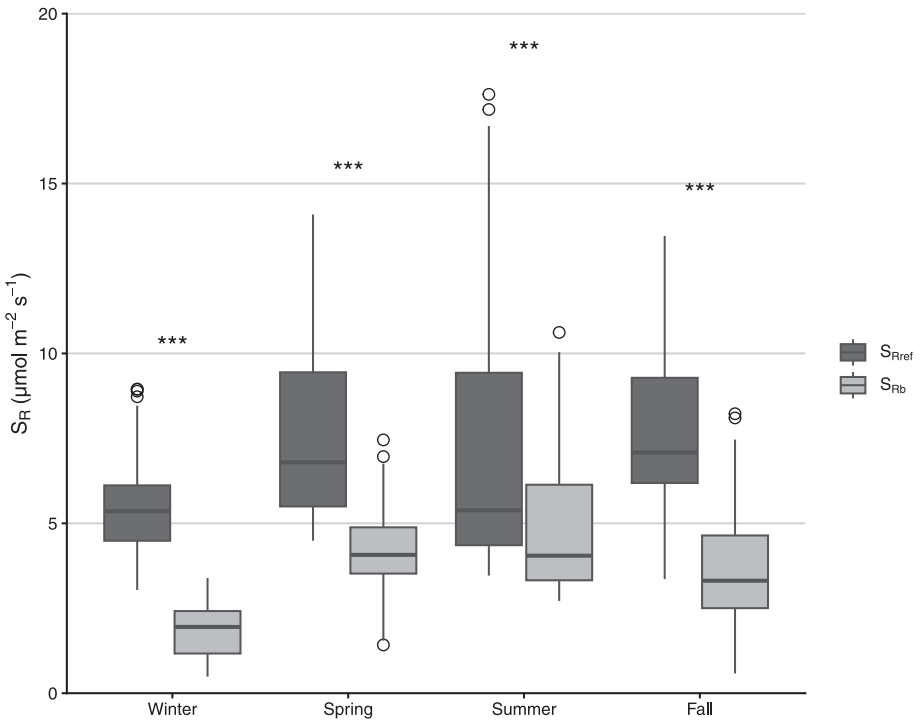

Fig. 7. Boxplots show the distribution of daily mean soil respiration rates with (S_{Rref}) and without (S_{Rb}) litter (µmol m^2 s^{-1}) for each season (Winter, Spring, Summer, and Fall). The central line indicates the median; boxes represent the interquartile range (IQR), whiskers extend to 1.5 × IQR, and dots denote outliers. The asterisks indicate significant seasonal variations between S_{Rref} and S_{Rb}.

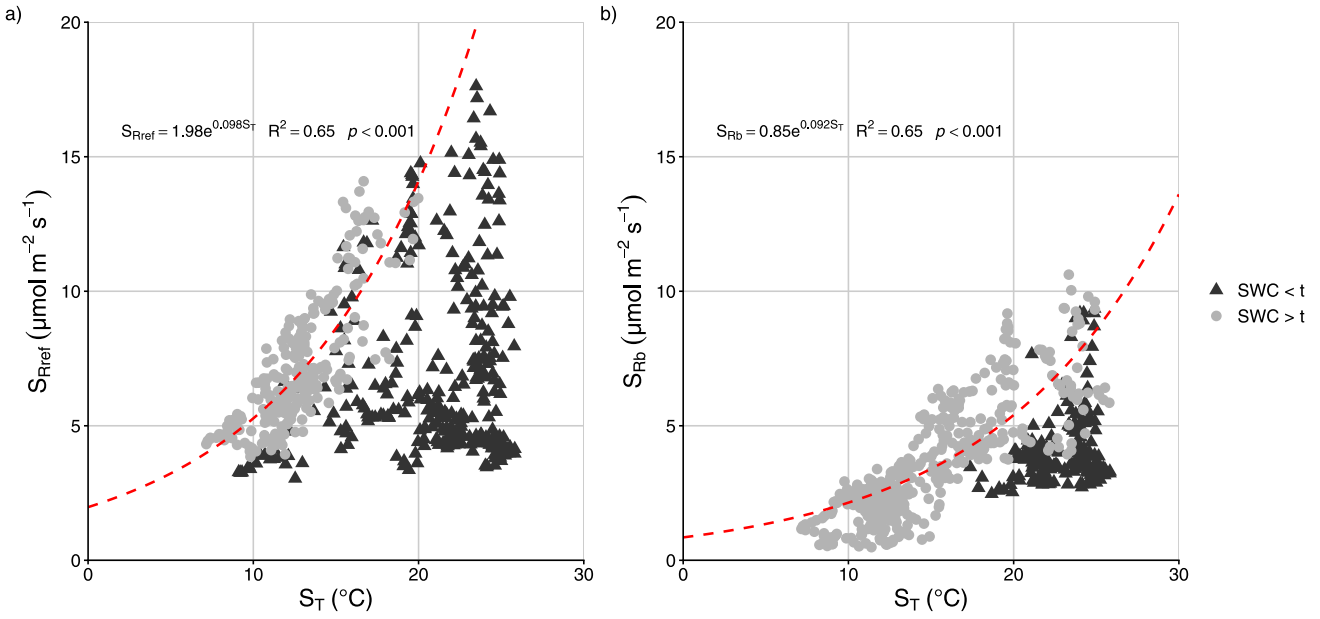

Fig. 8. Determination of Q_{10} derived from the exponential relationship between reference soil respiration (S_{Rref}, left panel) or respiration of bare soil (S_{Rb}, right panel) and soil temperature (S_T). Data were distinguished based on SWC thresholds (see 2.3.1 paragraph): light grey circles indicate data filtered for SWC above the identified threshold (THR_{SWC}); dark grey triangles indicate data filtered for SWC below the identified threshold (thresholds: $S_{Rref} = 10.6$; $S_{Rb} = 7.5$). Equation and fit shown in the graphs are related to data filtered for SWC ≥ THR_{SWC}. Overall exponential fits are shown in Table 2.

SWC values between 4% and 7%, that marked the transition from temperature-controlled to moisture-controlled respiration across different tree-decline stages.

The importance of using moisture thresholds to understand soil respiration has also been highlighted by Lellei-Kovács et al. (2011), who identified SWC values around 7.0–9.1% as the point at which moisture was no longer limiting for plant and microbial activity in their semiarid forest-steppe experiment. They noted that this threshold corresponded roughly to the field capacity of their site, where excess water can reduce measurable CO_2 efflux by promoting its dissolution in soil water. Similarly, He et al. (2024) identified a 12.45% SWC threshold, representing 75–80% of field capacity (FC), interpreting it as the point where capillary water shifts from continuous to discontinuous. Consistently, at our experimental site the identified threshold (~10%), corresponds to

Table 2
Apparent temperature sensitivity (Q_{10}) of soil respiration under litter-covered reference conditions (S_{Rref}) and bare-soil conditions after litter removal (S_{Rb}).

Respiration type	Filter	R^2	Q_{10}	No. of daily records	*p*
S_{Rref}	all data	R^2 = 0.02	1.11	620	*0.05*
	SWC > 10.6	R^2 = 0.65	2.66	258	*0.001*
	SWC < 10.6	R^2 = 0.01	n.s.	362	0.141
	all data	R^2 = 0.31	1.7	631	*0.001*
	SWC > 7.5	R^2 = 0.65	2.51	422	*0.001*
S_{Rb}	SWC < 7.5	R^2 = 0.04	1.43	209	*0.05*

Relationships between daily mean soil respiration and soil temperature were fitted using all available data and filtering observations according to the treatment-specific SWC thresholds. R^2, Q_{10} values, number of daily observations, and *p*-values are reported for each fit. The number of daily observations indicates the daily mean S_R values included in each regression. "n.s." indicates that the exponential fit was not statistically significant.

approximately 70–75% of FC (14.13%), as calculated using the Saxton equations (Saxton et al., 1986) for the sandy soil at the IT-Cp2 Flux site (Pinzari et al., 1999; Biondi et al., 2001). The observed proximity between the THR_{SWC} and the FC suggests that expressing thresholds as fractions of FC may offer a more generalizable approach, linking soil moisture responses to soil textural properties rather than absolute SWC values. Our modelling approach, based on a simple temperature response modulated by soil water content, was able to reproduce both the magnitude and temporal variability of soil respiration over multiple years. Despite relying only on easily measurable drivers (soil temperature and SWC) and a limited number of site-specific parameters, the model captured a substantial fraction of the variance in both reference and bare soil respiration and reproduced the main seasonal patterns. This level of agreement is comparable to that reported for more complex models that explicitly separate multiple soil carbon pools or include detailed descriptions of autotrophic and heterotrophic components (e.g. Rey et al., 2002; Zhuang et al., 2023; Curiel Yuste et al., 2003). However, the rainfall-pulse domain showed a lower explanatory power than the dry and moist hydro-thermal regimes. This result should not be interpreted only as a limitation of the modelling approach, but also as an indication of the intrinsically transient and heterogeneous nature of post-rainfall CO_2 efflux in Mediterranean soils (Matteucci et al., 2015). Rewetting after dry periods can induce short-lived respiration pulses whose magnitude and duration depend not only on daily SWC and S_T, but also on antecedent drought intensity, rainfall amount and timing, wetting depth, substrate availability, and microbial and rhizosphere reactivation (Li et al., 2018; Patel et al., 2021). The relatively low model performance highlights the need for additional event-based predictors, including antecedent dry-period length, rainfall amount and intensity, time since rainfall (Manzoni et al., 2020).

4.2. Temperature sensitivity of soil respiration

The analysis of temperature sensitivity provides further evidence for a threshold-mediated regulation of soil respiration. Both reference soil respiration and bare soil respiration exhibited strong and significant temperature dependence only when soil water content exceeded the identified thresholds, as indicated by high Q_{10} values (2.66 for S_{Rref} and 2.51 for S_{Rb}) and substantial explained variance (R^2 = 0.65 in both cases). In contrast, under moisture-limited conditions, Q_{10} values were low or not significant, and the relationship between S_R and S_T largely collapsed, indicating that temperature sensitivity is strongly constrained by soil dryness. This interpretation is consistent with the Q_{10}-SWC pattern shown in Fig. 9, where apparent Q_{10} generally increased with increasing SWC. Below the model-derived breakpoint (~9.6% SWC), apparent Q_{10} increased steeply with soil moisture, suggesting that even small increases in water availability substantially enhance the responsiveness of soil respiration to temperature. Above this threshold, the Q_{10} - SWC relationship became markedly weaker, indicating that once a minimum moisture requirement is met, additional water no longer

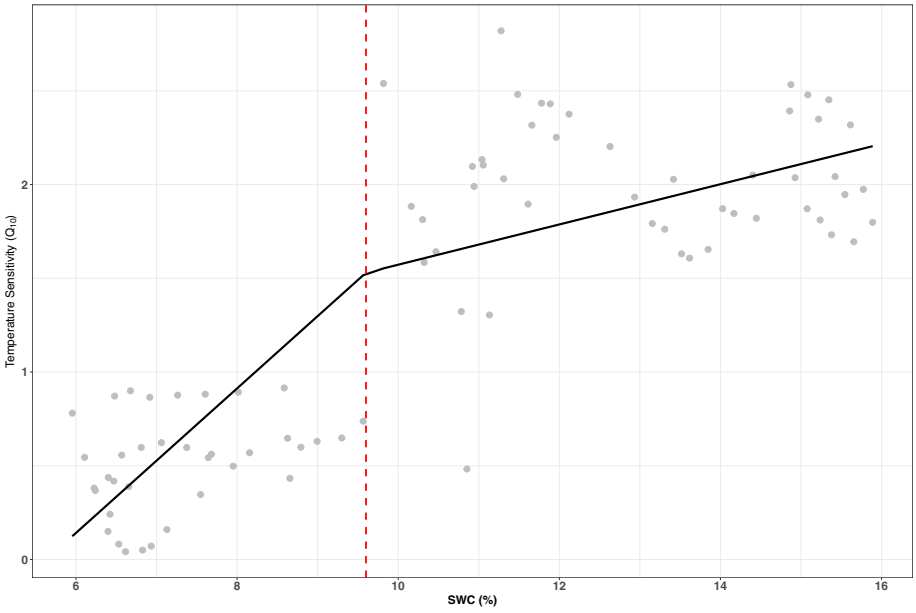

Fig. 9. Relationship between apparent temperature sensitivity (Q_{10}), estimated using two-month moving windows, and mean soil water content (SWC). The vertical red dashed line indicates the SWC threshold of 9.6% identified by the general soil respiration model and used here as a reference to distinguish moisture regimes. Fitted lines are shown as descriptive visual aids. When this model-derived threshold is superimposed on the moving-window Q_{10} estimates, the pattern is consistent with a moisture-dependent response tending toward saturation. Under low SWC, apparent Q_{10} tends to increase more markedly with increasing soil water availability, whereas above the threshold the relationship becomes weaker, suggesting that additional moisture exerts a smaller control on temperature sensitivity once dry-soil limitation is alleviated. (For interpretation of the references to colour in this figure legend, the reader is referred to the web version of this article.)

strongly modulates temperature sensitivity. Together, these results indicate a transition from a moisture-limited regime, in which soil respiration is weakly responsive to temperature, to a temperature-dominated regime, in which thermal control becomes fully expressed (Yuste et al., 2003; Chang et al., 2014).

This pattern indicates that soil moisture strongly modulates the apparent temperature sensitivity of soil respiration, particularly under dry conditions when microbial activity and substrate diffusion are most constrained. Similar threshold-like or decoupling behaviors have been reported across a range of ecosystems. For instance, Lellei-Kovács et al. (2011) observed distinct moisture thresholds in the temperature response of soil respiration in a semi-arid grassland, with strong interactive effects of soil drying on Q_{10}. In Mediterranean and temperate forest ecosystems, summer drought has been shown to weaken the coupling between soil temperature and respiration, leading to reduced apparent Q_{10} despite high temperatures (Rey et al., 2002; Yuste et al., 2003).

More recent studies have further demonstrated non-linear and moisture-dependent Q_{10} responses, including moisture optima and long-term modulation by interacting environmental drivers (He et al., 2024). Our findings add to this body of evidence by showing that the model-derived SWC threshold corresponds to a coherent change in the apparent temperature sensitivity of soil respiration.

Accordingly, the Q_{10} - SWC relationship provides diagnostic support for the threshold-based interpretation, as change in temperature sensitivity reflects transitions between moisture and temperature-limited regimes. However, Q_{10} values derived under field conditions should be interpreted as apparent sensitivities integrating not only temperature, but also moisture, substrate availability, root activity, and seasonal biological dynamics. This approach enables a mechanistic representation of temperature-moisture interactions controlling soil respiration, while keeping model complexity low compared with process-based approaches.

4.3. Differences between reference and bare-soil respiration

Reference soil respiration (S_{Rref}) consistently exceeded bare-soil respiration (S_{Rb}), confirming the additional contribution of surface litter presence to total soil CO_2 efflux. This pattern is consistent with previous studies showing that heterotrophic processes can represent a substantial fraction, for 30–60% of total soil CO_2 efflux, of total soil respiration in forest ecosystems (Sulzman et al., 2005; Ferréa et al., 2012). However, since S_{Rb} does not represent purely autotrophic respiration, the difference between S_{Rref} and S_{Rb} is interpreted as a surface-litter-related contribution to soil CO_2 efflux, rather than as a full partitioning between autotrophic and heterotrophic respiration. The seasonal boxplots further demonstrate that S_{Rref} exceeded S_{Rb} consistently across all seasons, with the largest differences observed during spring and autumn. This seasonal amplification suggests that litter-associated processes intensify soil CO_2 efflux when temperature and moisture conditions favor microbial activity. Moreover, the greater variability of S_{Rref} indicates that the litter layer enhances pulse-driven dynamics, particularly during transitional seasons (Zacharoudi et al., 2025). In contrast, S_{Rb} displayed a narrower distribution and a more stable seasonal pattern, consistent with the removal of the highly variable surface-litter component and with a stronger influence of mineral-soil and root-related processes. The lower THR_{SWC} observed for S_{Rb} compared with S_{Rref}, indicates that, after litter removal, the transition toward more temperature-responsive respiration occurred under drier soil conditions. A plausible interpretation, supported by previous litter-manipulation studies (Fuentes et al., 2014; Han et al., 2019), is that removing the surface litter layer reduced near-surface moisture retention and labile substrate availability, while exposing the mineral soil more directly to atmospheric drying and warming. Conversely, under S_{Rref} conditions, the litter layer may buffer short-term hydro-thermal fluctuations and provide decomposable substrates. However, in this Mediterranean forest dominated by *Q. ilex*, where litter is characterized by slow-decomposing sclerophyll leaves (Incerti et al., 2011), the litter-associated respiratory component may require higher moisture levels to become fully activated after dry periods. This interpretation is consistent with the higher threshold observed under litter-covered conditions, although the relative contribution of moisture buffering, thermal effects, substrate availability, and litter rewetting dynamics cannot be fully separated with our experimental design

Together, these patterns indicate that litter presence modifies not only the magnitude but also the seasonal amplitude and environmental sensitivity of soil respiration, reinforcing the need to consider component-specific controls rather than relying on aggregated temperature response functions. This interpretation is also supported by the temperature-sensitivity analysis (Table 2).Across the full dataset, S_{Rb} showed a higher apparent temperature sensitivity than S_{Rref} ($Q_{10} = 1.7$ vs. 1.11), suggesting that, after surface litter removal, soil CO_2 efflux was more directly coupled to temperature, also as a consequence of the tight coupling of root-derived CO_2 efflux to canopy photosynthesis and carbon allocation documented by girdling experiments (e.g. Subke et al., 2011). In contrast, the inclusion of the litter layer in S_{Rref} introduces additional surface processes that are strongly influenced by soil moisture and pulse dynamics, thereby weakening a simple temperature respiration relationship when data are pooled across seasons. Moreover, litter removal can alter soil microclimatic conditions, including temperature amplitude and moisture buffering (Walkiewicz et al., 2021), further contributing to differences in apparent temperature sensitivity.

Moisture-stratified fits confirmed this interpretation: under non-limiting soil water content, both fluxes exhibited similarly high temperature sensitivity (Q_{10} of 2.5 and 2.7 for S_{Rb} and S_{Rref}, respectively), whereas under dry conditions S_{Rref} was decoupled from temperature (Table 2), indicating a shift toward moisture limitation and reduced predictability from soil temperature alone. Overall, litter increases the moisture dependence of S_{Rref} and limits the expression of temperature sensitivity under dry conditions. Experimental manipulations have shown that litter addition enhances soil CO_2 efflux by increasing the supply of labile carbon and stimulating microbial activity, whereas litter removal can reduce respiration by 20–40% depending on forest type (Sayer et al., 2011; Chen et al., 2014). These effects might be more pronounced in holm oak forests characterized by litter with a high lignin content and low decomposability. As reported by Vitale et al. (2019) litter decomposition of *Q. ilex* showed lower mass loss rates when compared to other oak species, with only a 25% mass loss compared with 40% in *Q. pubescens* and 42% in *Q. robur*, and showed the highest lignin accumulation (+91% vs. +69% and + 57%), confirming its greater recalcitrance. Together, these patterns indicate that surface litter presence modifies not only the magnitude of soil CO_2 efflux, but also its seasonal amplitude, moisture dependence, and apparent temperature sensitivity. This reinforces the need to consider surface-litter-related controls when interpreting spatial and temporal patterns of soil respiration, rather than relying on a single aggregated temperature–moisture response function for the whole soil system.

4.4. Strengths, limitations and future perspectives

A key strength of this study is the combination of continuous high-frequency automated chamber measurements with a data-driven threshold modelling framework under natural Mediterranean field conditions. The multi-year dataset allowed us to capture seasonal transitions, drought periods, and post-rainfall responses that are difficult to resolve with conventional spot measurements. In addition, the paired litter-removal comparison provided insight into how surface litter presence modifies both the magnitude of soil CO_2 efflux and its hydro-thermal sensitivity. Rather than imposing predefined moisture classes, the modelling approach identified site-specific SWC and rainfall thresholds directly from the data, allowing soil respiration to be interpreted across functionally distinct response domains. This combination

of continuous monitoring, experimental litter manipulation, and low-complexity threshold modelling, represents a robust site-calibrated approach that can be conceptually applied to other seasonally water-limited ecosystems.

Some limitations relative to spatial representativeness, model generalization, and experimental assumptions should also be acknowledged to better define the scope of our findings. Although chambers were installed within the ICOS Continuous Plots to capture representative soil respiration dynamics within the tower footprint, the number of automated chambers may result limited and therefore, small-scale spatial heterogeneity in root distribution, litter accumulation, soil structure, and microsite conditions may not be fully represented. A second limitation concerns the extrapolation of the identified threshold. The thresholds derived in this study reflect the site-specific interplay of soil texture, moisture regime, and species composition. In this Mediterranean ecosystem, the dominance of sclerophyll species shapes litter quality, resulting in structurally complex, thus constraining decomposition processes and soil respiration dynamics. Therefore, the resulting thresholds and parameterization should not be considered universally applicable but rather interpreted as site-specific. Rather, its proximity to field capacity suggests that moisture thresholds may be more robustly defined relative to site-specific soil hydraulic properties than as absolute SWC values. With automated long-term chamber measurements are increasingly being implemented across ICOS network sites, future applications in contrasting ecosystems could test this hypothesis more broadly.

Model performance also varied across response domains. The rainfall-pulse domain showed lower predictive ability than the dry and moist hydro-thermal regimes, reflecting the short-lived and event-specific nature of post-rainfall CO_2 pulses. Future developments should aim to integrate event-based descriptors that capture the inherent complexity of post-rainfall respiration dynamics. Finally, the litter-removal comparison did not allow for the full partitioning between autotrophic and heterotrophic respiration, but it enabled to estimate the litter contribution to soil CO_2 fluxes, mainly associated with litter presence and decomposition. We also observed that the exclusion of litter modified the moisture level at which soil respiration shifted from moisture-limited to more temperature-responsive conditions. However, chamber-specific microclimatic differences cannot be entirely excluded, as S_T and SWC were not measured within the paired S_{Rref} and S_{Rb} collars. Given that the chambers were co-located within the same CPs, we assumed such differences to be negligible, attributing the observed effects primarily to litter exclusion.

Although the model captured a substantial proportion of S_R variability under both dry and moist conditions, some discrepancies remained. In particular, the recurrent underestimation observed under hot and dry or partially rewetted conditions, highlights the need to incorporate additional controls beyond micrometeorological variables, in order to better represent S_R dynamics beyond the dominant hydro-thermal controls.

5. Conclusions

This study demonstrates that soil respiration in a Mediterranean forest is governed by a threshold-mediated interaction between soil temperature and soil water content. A distinct transition from moisture limitation to temperature control emerged when soil water content exceeded approximately 10%, a value close to the estimated field capacity of the soil. While the absolute threshold is site-specific, its consistent proximity to field capacity indicates that this transition is constrained by a physically defined hydrological boundary rather than by arbitrary local conditions. Similar moisture-dependent shifts reported across contrasting ecosystems suggest that the activation of temperature sensitivity reflects a common functional reorganization of soil physical conditions, particularly pore connectivity and oxygen availability. Our results therefore identify soil field capacity as a critical reference point for understanding when soil respiration becomes fully temperature responsive. Our findings support the explicit representation of hydrological thresholds as boundary conditions for soil CO_2 fluxes. The observed proportionality with field capacity further suggests that expressing thresholds relative to local hydrological reference points may facilitate site-specific parameterization and comparison across ecosystems.

The increase in apparent Q_{10} with SWC further supports the central role of hydrological thresholds in regulating when temperature sensitivity becomes expressed under field conditions. While the threshold-based approach effectively distinguishes relatively stable dry and moist hydro-thermal regimes, short-lived rainfall-pulse responses were less well captured, indicating that additional event-based descriptors are needed to represent soil respiration driven by rapid rewetting dynamics.

Although derived from a single long-term site, this approach can be applied to other seasonally water-limited ecosystems after local calibration. Such an approach is especially relevant for Mediterranean ecosystems, where increasing drought frequency is expected to strengthen hydrological controls on soil-atmosphere carbon exchange and influence regional carbon climate feedbacks.

Declaration of generative AI and AI-assisted technologies in the manuscript preparation process

During the preparation of this work the authors used ChatGPT in order to finalize the graphical abstract of the manuscript. After using this tool/service, the authors reviewed and edited the content as needed and take full responsibility for the content of the published article.

CRediT authorship contribution statement

Lina Fusaro: Writing – review & editing, Writing – original draft, Methodology, Investigation, Formal analysis, Conceptualization. **Adriano Conte:** Writing – review & editing, Writing – original draft, Methodology, Investigation, Formal analysis, Conceptualization. **Carlotta Ferrara:** Writing – review & editing, Methodology, Formal analysis. **Tiziano Sorgi:** Investigation. **Roberto Corsanici:** Investigation, Formal analysis. **Silvano Fares:** Writing – review & editing, Supervision, Funding acquisition, Conceptualization.

Declaration of competing interest

The authors declare that they have no known competing financial interests or personal relationships that could have appeared to influence the work reported in this paper.

Acknowledgments

This study was supported by: P@CNR_01_BIOCITY, CUP B85F21006360005; National Recovery and Resilience Plan (NRRP), Mission 4 Component 2 Investment 1.4 - Call for tender No. 3138 of December 16, 2021, rectified by Decree n.3175 of December 18, 2021 of Italian Ministry of University and Research funded by the European Union – NextGenerationEU. Award Number: Project code CN_00000033, Concession Decree No. 1034 of June 17, 2022 adopted by the Italian Ministry of University and Research, CUP B83C22002950007, Project title “National Biodiversity Future Center - NBFC”. The research was also made possible thanks to the following: the Scientific Commission of Castelporziano and the Multi-disciplinary Center for the Study of Coastal Mediterranean Ecosystems. We thank ICOS ETC for providing the elaborated ancillary data for site It-Cp2.

Appendix A. Supplementary data

Supplementary data to this article can be found online at https://doi.org/10.1016/j.catena.2026.110457.

Data availability

The Authors declare that the data supporting this study's findings are provided within the manuscript or supplementary information files, and further information can be requested from the corresponding author upon reasonable request.

References

Almagro, M., López, J., Querejeta, J.I., Martínez-Mena, M., 2009. Temperature dependence of soil CO_2 efflux is strongly modulated by seasonal patterns of moisture availability in a Mediterranean ecosystem. Soil Biol. Biochem. 41, 594–605. https://doi.org/10.1016/j.soilbio.2008.12.024.

Almagro, M., Rey, A., Inclán, R.M., Barba, J., Vargas, R., Carrara, A., et al., 2025. Vegetation type and climate determine temperature thresholds of soil respiration across drylands. Soil Biol. Biochem. 190, 109984. https://doi.org/10.1016/j.soilbio.2024.109984.

Aranda-Barranco, S., Serrano-Ortiz, P., Kowalski, A.S., Sánchez-Cañete, E.P., 2025. Spatial and temporal heterogeneity of soil respiration in a bare-soil Mediterranean olive grove. Soil 11, 213–232. https://doi.org/10.5194/soil-11-213-2025.

Biondi, F.A., Dowgiallo, G., Gisotti, G., Tinelli, A., Figliola, A., Scarascia Mugnozza, G., 2001. Memoria illustrativa della carta dei suoli della Tenuta di Castelporziano. In: Il Sistema Ambientale della Tenuta Presidenziale di Castelporziano. Ricerche sulla complessità di un ecosistema forestale costiero mediterraneo.

Bond-Lamberty, B., Wang, C., Gower, S.T., 2004. A global relationship between the heterotrophic and autotrophic components of soil respiration? Glob. Chang. Biol. 10, 1756–1766. https://doi.org/10.1111/j.1365-2486.2004.00816.x.

Bond-Lamberty, B., Ballantyne, A., Berryman, E., Fluet-Chouinard, E., Jian, J., Morris, K. A., Vargas, R., 2024. Twenty years of progress, challenges, and opportunities in measuring and understanding soil respiration. J. Geophys. Res. Biogeosci. 129. https://doi.org/10.1029/2023JG007637 e2023JG007637.

Brændholt, A., Ibrom, A., Larsen, K.S., Pilegaard, K., 2018. Partitioning of ecosystem respiration in a beech forest. Agric. For. Meteorol. 252, 88–98. https://doi.org/10.1016/j.agrformet.2018.01.012.

Cai, Y., Sawada, K., Hirota, M., 2023. Spatial variation in forest soil respiration: a systematic review of field observations at the global scale. Sci. Total Environ. 874, 162348. https://doi.org/10.1016/j.scitotenv.2023.162348.

Chang, C.-T., Sabaté, S., Sperlich, D., Poblador, S., Sabater, F., Gracia, C., 2014. Does soil moisture override temperature dependence of soil respiration in Mediterranean riparian forests? Biogeosciences 11, 6173–6185. https://doi.org/10.5194/bg-11-6173-2014.

Chang, C.T., Sperlich, D., Sabaté, S., Sánchez-Costa, E., Cotillas, M., Espelta, J.M., et al., 2016. Mitigating the stress of drought on soil respiration by selective thinning: contrasting effects of drought on soil respiration of two oak species in a Mediterranean forest. Forests 7, 263. https://doi.org/10.3390/f7110263.

Chen, J., Luo, Y., Xia, J., Shi, Z., Jiang, L., Niu, S., et al., 2014. Stronger warming effects on microbial than root respiration in terrestrial ecosystems. Glob. Chang. Biol. 20, 255–268. https://doi.org/10.1111/gcb.12330.

Conte, A., Fares, S., Salvati, L., Savi, F., Matteucci, G., Mazzenga, F., et al., 2019. Ecophysiological responses to rainfall variability in grassland and forests along a latitudinal gradient in Italy. Front. For. Glob. Change 2, 16. https://doi.org/10.3389/ffgc.2019.00016.

Dacal, M., Delgado-Baquerizo, M., Barquero, J., Berhe, A.A., Gallardo, A., Maestre, F.T., García-Palacios, P., 2022. Temperature increases soil respiration across ecosystem types and soil development, but soil properties determine the magnitude of this effect. Ecosystems 25, 184–198. https://doi.org/10.1007/s10021-021-0064.

Du, Y., Wang, Y.P., Hui, D., Su, F., Yan, J., 2023. Significant effects of precipitation frequency on soil respiration and its components—a global synthesis. Glob. Chang. Biol. 29, 1188–1205. https://doi.org/10.1111/gcb.16532.

Fares, S., Alivernini, A., Chianucci, F., Conte, A., Corsanici, R., Ilardi, F., Moretti, V., Sorgi, T., 2025. ETC L2 Fluxnet (half-hourly) from Castelporziano2, 2020-12-31–2025-09-30 [dataset]. ICOS RI. https://hdl.handle.net/11676/pcYUl7GnWQTOLNL2RZ6lC6EP.

Ferréa, C., Zenone, T., Comolli, R., Seufert, G., 2012. Estimating heterotrophic and autotrophic soil respiration in a semi-natural forest of Lombardy, Italy. Pedobiologia 55, 285–294. https://doi.org/10.1016/j.pedobi.2012.05.001.

Franz, D., Acosta, M., Altimir, N., Arriga, N., Arrouays, D., Aubinet, M., Cescatti, A., Elbers, J.A., Eugster, W., Gioli, B., Grünwald, T., Heinesch, B., Janssens, I.A., Knohl, A., Laurila, T., Mammarella, I., Merbold, L., Montagnani, L., Papale, D., Pilegaard, K., Rebmann, C., Saunders, M., Vesala, T., 2018. Towards long-term standardised carbon and greenhouse gas observations for monitoring Europe's terrestrial ecosystems: a review. Int. Agrophys. 32, 439–455. https://doi.org/10.1515/intag-2017-0039.

Fuentes, J.P., Bown, H.E., Perez-Quezada, J.F., Franck, N., 2014. Litter removal in a sclerophyll forest: short- and medium-term consequences for soil properties. Soil Sci. Soc. Am. J. 78, 634–644. https://doi.org/10.2136/sssaj2013.03.0100.

Gielen, B., Op de Beeck, M., Michilsens, F., Papale, D., 2017a. ICOS Ecosystem Instructions for Ancillary Vegetation Measurements in Forest (Version 20200330) [Report]. ICOS Ecosystem Thematic Centre. https://doi.org/10.18160/4ajs-z4r9.

Fusaro, L., Salvatori, E., Manes, F., 2017. Effects of nitrogen deposition, drought and their interaction on functional and structural traits of Fraxinus ornus L. and Quercus ilex L. Plant Biosyst 151, 174–189.

Fusaro, L., Salvatori, E., Mereu, S., Silli, V., Bernardini, A., Tinelli, A., Manes, F., 2015. Researches in Castelporziano test site: Ecophysiological studies on Mediterranean vegetation in a changing environment. Rend. Lincei 26, 473–481.

Gielen, B., Op de Beeck, M., Loustau, D., Ceulemans, R., Jordan, A., Papale, D., 2017b. Integrated carbon observation system (ICOS): An infrastructure to monitor the European greenhouse gas balance. In: Terrestrial Ecosystem Research Infrastructures. CRC Press, pp. 505–520.

González-Ubierna, S., Lai, R., 2019. Modelling the effects of climate factors on soil respiration across Mediterranean ecosystems. J. Arid Environ. 165, 46–54. https://doi.org/10.1016/j.jaridenv.2019.02.008.

González-Ubierna, S., de la Cruz, M.T., Casermeiro, M.Á., 2014. Climate factors mediate soil respiration dynamics in Mediterranean agricultural environments: an empirical approach. Soil Res. 52, 543–553. https://doi.org/10.1071/SR14008.

Groemping, U., 2006. Relative importance for linear regression in R: the package relaimpo. J. Stat. Softw. 17, 1–27.

Han, T., Huang, W., Liu, J., Zhou, G., Xiao, Y., 2015. Different soil respiration responses to litter manipulation in three subtropical successional forests. Sci. Rep. 5, 18166. https://doi.org/10.1038/srep18166.

Han, C., Liu, T., Lu, X., Duan, L., Singh, V.P., Ma, L., 2019. Effect of litter on soil respiration in a man-made Populus L. forest in a dune-meadow transitional region in China's Horqin sandy land. Ecol. Eng. 127, 276–284. https://doi.org/10.1016/j.ecoleng.2018.12.005.

Hao, Y., Mao, J., Bachmann, C.M., Hoffman, F.M., Koren, G., Chen, H., et al., 2025. Soil moisture controls over carbon sequestration and greenhouse gas emissions: a review. Npj Clim. Atmos. Sci. 8, 16. https://doi.org/10.1038/s41612-024-00888-8.

Hastie, T.J., Pregibon, D., 1992. Generalized linear models. In: Chambers, J.M., Hastie, T. J. (Eds.), Statistical Models in S. Wadsworth & Brooks/Cole, Pacific Grove, CA.

He, H., Zha, T., Tan, J., 2024. Soil-moisture-dependent temperature sensitivity of soil respiration in a poplar plantation in northern China. Forests 15, 1466. https://doi.org/10.3390/f15081466.

Hu, S., Li, Y., Chang, S.X., Li, Y., Yang, W., Fu, W., et al., 2018. Soil autotrophic and heterotrophic respiration respond differently to land-use change and variations in environmental factors. Agric. For. Meteorol. 250–251, 290–298. https://doi.org/10.1016/j.agrformet.2018.01.003.

Incerti, G., Bonanomi, G., Giannino, F., Rutigliano, F.A., Piermatteo, D., Castaldi, S., Mazzoleni, S., 2011. Litter decomposition in Mediterranean ecosystems: modelling the controlling role of climatic conditions and litter quality. Appl. Soil Ecol. 49, 148–157. https://doi.org/10.1016/j.apsoil.2011.06.004.

Johnston, A.S., Sibly, R.M., 2018. The influence of soil communities on the temperature sensitivity of soil respiration. Nat. Ecol. Evol. 2 (10), 1597–1602. https://doi.org/10.1038/s41559-018-0648-6.

Kuzyakov, Y., Gavrichkova, O., 2010. Time lag between photosynthesis and carbon dioxide efflux from soil: A review of mechanisms and controls. Glob. Change Biol. 16, 3386–3406.

Lellei-Kovács, E., Botta-Dukát, Z., De Dato, G., Estiarte, M., Guidolotti, G., Kopittke, G.R., et al., 2016. Temperature dependence of soil respiration modulated by thresholds in soil water availability across European shrubland ecosystems. Ecosys 19, 1460–1477.

Lellei-Kovács, E., Kovács-Láng, E., Botta-Dukát, Z., Kalapos, T., Emmett, B., Beier, C., 2011. Thresholds and interactive effects of soil moisture on the temperature response of soil respiration. Eur. J. Soil Biol. 47, 247–255. https://doi.org/10.1016/j.ejsobi.2011.05.004.

Li, J.T., Wang, J.J., Zeng, D.H., Zhao, S.Y., Huang, W.L., Sun, X.K., Hu, Y.L., 2018. The influence of drought intensity on soil respiration during and after multiple drying-rewetting cycles. Soil Biol. Biochem. 127, 82–89. https://doi.org/10.1016/j.soilbio.2018.09.018.

Lindemann, R.H., Merenda, P.F., Gold, R.Z., 1990. Introduction to Bivariate and Multivariate Analysis. Scott, Foresman and Company, Glenview, IL.

Lionello, P., Malanotte-Rizzoli, P., Boscolo, R., Alpert, P., Artale, V., Li, L., et al., 2006. The Mediterranean climate: an overview of the main characteristics and issues. Dev. Earth Environ. Sci. 4, 1–26. https://doi.org/10.1016/S1571-9197(06)80003-0.

Manzoni, S., Chakrawal, A., Fischer, T., Schimel, J.P., Porporato, A., Vico, G., 2020. Rainfall intensification increases the contribution of rewetting pulses to soil heterotrophic respiration. Biogeosciences 17 (15), 4007–4023. https://doi.org/10.5194/bg-17-4007-2020.

Matteucci, M., Gruening, C., Ballarin, I.G., Seufert, G., Cescatti, A., 2015. Components, drivers and temporal dynamics of ecosystem respiration in a Mediterranean pine forest. Soil Biol. Biochem. 88, 224–235. https://doi.org/10.1016/j.soilbio.2015.05.017.

Miles, J., 2014. Tolerance and variance inflation factor. In: Wiley StatsRef: Statistics Reference Online. Wiley. https://doi.org/10.1002/9781118445112.stat06593.

Morote, F.A.G., Abellán, M.A., Rubio, E., García, E.M., Saucedo, F.G., Córdoba, M.I.P., Serrano, F.R.L., 2022. Productivity and seasonality drive total soil respiration in semi-arid Juniper woodlands (*Juniperus thurifera* L., southern Spain). Forests 13, 538. https://doi.org/10.3390/f13040538.

Ngaba, M.J.Y., Uwiragiye, Y., Hu, B., Zhou, J., Dannenmann, M., Calanca, P., Rennenberg, H., 2024. Effects of environmental changes on soil respiration in arid, cold, temperate, and tropical zones. Sci. Total Environ. 952, 175943. https://doi.org/10.1016/j.scitotenv.2024.175943.

Otu-Larbi, F., Bolas, C.G., Ferracci, V., Staniaszek, Z., Jones, R.L., Malhi, Y., et al., 2020a. Modelling the effect of the 2018 summer heatwave and drought on isoprene emissions in a UK woodland. Glob. Chang. Biol. 26, 2320–2335. https://doi.org/10.1111/gcb.14963.

Otu-Larbi, F., Conte, A., Fares, S., Wild, O., Ashworth, K., 2020b. Current and future impacts of drought and ozone stress on northern hemisphere forests. Glob. Chang. Biol. 26, 6218–6234. https://doi.org/10.1111/gcb.15339.

Oyonarte, C., Rey, A., Raimundo, J., Miralles, I., Escribano, P., 2012. The use of soil respiration as an ecological indicator in arid ecosystems of southeastern Spain: spatial variability and controlling factors. Ecol. Indic. 14, 40–49. https://doi.org/10.1016/j.ecolind.2011.08.013.

Papale, D., Nicolini, G., 2016. ICOS ecosystem Instructions for Setting Up the Spatial Sampling Scheme (Version 20170802) [Report]. ICOS Ecosystem Thematic Centre. https://doi.org/10.18160/c5q7-z877.

Patel, K.F., Myers-Pigg, A.N., Bond-Lamberty, B., Fansler, S.J., Norris, C.G., McKever, S. A., Zheng, J., Rod, K.A., Bailey, V.L., 2021. Soil carbon dynamics during drying vs. rewetting: importance of antecedent moisture conditions. Soil Biol. Biochem. 156, 108165. https://doi.org/10.1016/j.soilbio.2021.108165.

Pavelka, M., Acosta, M., Kiese, R., Altimir, N., Brümmer, C., Crill, P., et al., 2018. Standardisation of chamber technique for CO_2, N_2O and CH_4 flux measurements from terrestrial ecosystems. Int. Agrophys. 32, 569–587.

Phillips, C.L., Bond-Lamberty, B., Desai, A.R., Lavoie, M., Risk, D., Tang, J., Vargas, R., 2017. The value of soil respiration measurements for interpreting and modeling terrestrial carbon cycling. Plant Soil 413, 1–25. https://doi.org/10.1007/s11104-016-3084-x.

Pinzari, F., Trinchera, A., Benedetti, A., Sequi, P., 1999. Use of biochemical indices in the Mediterranean environment: comparison among soils under different forest vegetation. J. Microbiol. Methods 36, 21–28. https://doi.org/10.1016/S0167-7012(99)00007-X.

R Core Team, 2025. R: A language and environment for statistical computing [software]. R Foundation for Statistical Computing, Vienna, Austria. https://www.R-project.org/.

Reichstein, M., Rey, A., Freibauer, A., Tenhunen, J., Valentini, R., Banza, J., Dolman, A. J., Dore, S., Gerbig, C., Grünzweig, J.M., Kutsch, W., Kurbatova, J., Yakir, D., 2003. Modeling temporal and large-scale spatial variability of soil respiration from soil water availability, temperature, and vegetation productivity indices. Glob. Biogeochem. Cycles 17, 1104. https://doi.org/10.1029/2003GB002035.

Rey, A., Pegoraro, E., Tedeschi, V., De Parri, I., Jarvis, P.G., Valentini, R., 2002. Annual variation in soil respiration and its components in a coppice oak forest in Central Italy. Glob. Chang. Biol. 8, 851–866. https://doi.org/10.1046/j.1365-2486.2002.00521.x.

Rodríguez, A., Durán, J., Yuste, J.C., Valladares, F., Rey, A., 2023. The effect of tree decline over soil water content largely controls soil respiration dynamics in a Mediterranean woodland. Agric. For. Meteorol. 333, 109398. https://doi.org/10.1016/j.agrformet.2023.109398.

Saxton, K.E., Rawls, W.J., Romberger, J.S., Papendick, R.I., 1986. Estimating generalized soil-water characteristics from texture. Soil Sci. Soc. Am. J. 50, 1031–1036. https://doi.org/10.2136/sssaj1986.03615995005000040039x.

Sayer, E.J., Heard, M.S., Grant, H.K., Marthews, T.R., Tanner, E.V.J., 2011. Soil carbon release enhanced by increased tropical forest litterfall. Nat. Clim. Chang. 1, 304–307. https://doi.org/10.1038/nclimate1190.

Shapiro, S.S., Wilk, M.B., 1965. An analysis of variance test for normality (complete samples). Biometrika 52, 591–611. https://doi.org/10.1093/biomet/52.3-4.591.

Storm, I., Karstens, U., D'Onofrio, C., Vermeulen, A., Peters, W., 2023. A view of the European carbon flux landscape through the lens of the ICOS atmospheric observation network. Atmos. Chem. Phys. 23, 4993–5008. https://doi.org/10.5194/acp-23-4993-2023.

Subke, J.-A., Heinemeyer, A., Reichstein, M., 2010. Experimental design: Scaling up in time and space, and its statistical considerations. In: Kutsch, W.L., Bahn, M., Heinemeyer, A. (Eds.), Soil Carbon Dynamics: An Integrated Methodology. Cambridge University Press, Cambridge, pp. 34–48. https://doi.org/10.1017/CBO9780511711794.004.

Subke, J.A., Voke, N.R., Leronni, V., Garnett, M.H., Ineson, P., 2011. Dynamics and pathways of autotrophic and heterotrophic soil CO_2 efflux revealed by forest girdling. J. Ecol. 99, 186–193. https://doi.org/10.1111/j.1365-2745.2010.01740.x.

Sulzman, E.W., Brant, J.B., Bowden, R.D., Lajtha, K., 2005. Contribution of aboveground litter, belowground litter, and rhizosphere respiration to total soil CO_2 efflux in an old-growth coniferous forest. Biogeochemistry 73, 231–256. https://doi.org/10.1007/s10533-004-7314-6.

Tang, X., Pei, X., Lei, N., Luo, X., Liu, L., Shi, L., et al., 2020. Global patterns of soil autotrophic respiration and its relation to climate, soil and vegetation characteristics. Geoderma 369, 114339. https://doi.org/10.1016/j.geoderma.2020.114339.

Tedeschi, V., Rey, A., Manca, G., Valentini, R., Jarvis, P.G., Borghetti, M., 2006. Soil respiration in a Mediterranean oak forest at different developmental stages after coppicing. Glob. Chang. Biol. 12, 110–121. https://doi.org/10.1111/j.1365-2486.2005.01092.x.

Venables, W.N., Ripley, B.D., 2002. Modern applied statistics with S, 4th ed. Springer, New York. https://doi.org/10.1007/978-0-387-21706-2.

Vitale, M., Amitrano, W., Hoshika, Y., Paoletti, E., 2019. Plant species-specific litter decomposition rates are directly affected by tropospheric ozone: Analysis of trends and modelling. Water Air Soil Pollut 230, 311.

Walkiewicz, A., Rafalska, A., Bulak, P., Bieganowski, A., Osborne, B., 2021. How can litter modify the fluxes of CO_2 and CH_4 from forest soils? A mini-review. Forests 12, 1276. https://doi.org/10.3390/f12091276.

Wang, C., Feng, X., 2025. Progress and perspective in parameterizing soil respiration responses to temperature and moisture. Sci. China Earth Sci. 1–18. https://doi.org/10.1007/s11430-024-1554-y.

Yan, T., Song, H., Wang, Z., Teramoto, M., Wang, J., Liang, N., Peng, S., 2019. Temperature sensitivity of soil respiration across multiple time scales in a temperate plantation forest. Sci. Total Environ. 688, 479–485. https://doi.org/10.1016/j.scitotenv.2019.06.318.

Yan, Y., Wang, J., Tian, D., Luo, Y., Xue, X., Peng, F., et al., 2022. Sustained increases in soil respiration accompany increased carbon input under long-term warming across global grasslands. Geoderma 428, 116157. https://doi.org/10.1016/j.geoderma.2022.116157.

Yuste, J.C., Janssens, I.A., Carrara, A., Meiresonne, L., Ceulemans, R., 2003. Interactive effects of temperature and precipitation on soil respiration in a temperate maritime pine forest. Tree Physiol. 23, 1263–1270. https://doi.org/10.1093/treephys/23.18.1263.

Zacharoudi, S., Fendrich, A., Cescatti, A., Spyroglou, G., Fotelli, M., Radoglou, K., Panagos, P., 2025. Monitoring and modelling soil respiration in deciduous and broadleaf evergreen oak-dominated ecosystems in Greece. Eur. J. Soil Sci. 76, e70254. https://doi.org/10.1111/ejss.70254.

Zhang, Z., Li, Y., Williams, R.A., Chen, Y., Peng, R., Liu, X., et al., 2023. Responses of soil respiration and its sensitivities to temperature and precipitation: a meta-analysis. Ecol. Inform. 75, 102057. https://doi.org/10.1016/j.ecoinf.2023.102057.

Zhuang, W., Liu, M., Wu, Y., Ma, J., Zhang, Y., Su, L., Fu, S., 2023. Litter inputs exert greater influence over soil respiration and its temperature sensitivity than roots in a coniferous forest in north-south transition zone. Sci. Total Environ. 886, 164009. https://doi.org/10.1016/j.scitotenv.2023.164009.

Zuur, A.F., Ieno, E.N., Elphick, C.S., 2010. A protocol for data exploration to avoid common statistical problems. Methods Ecol. Evol. 1, 3–14. https://doi.org/10.1111/j.2041-210X.2009.00001.x.